

# Online Research @ Cardiff

This is an Open Access document downloaded from ORCA, Cardiff University's institutional repository: <https://orca.cardiff.ac.uk/id/eprint/131077/>

This is the author's version of a work that was submitted to / accepted for publication.

Citation for final published version:

Blenkinsop, T. G. ORCID: <https://orcid.org/0000-0001-9684-0749>, Oliver, N. H. S., Dirks, P. G. H. M., Nugus, M., Tripp, G. and Sanislav, I. 2020. Structural geology applied to the evaluation of hydrothermal gold deposits. *Reviews in Economic Geology* 21 , pp. 1-23. 10.5382/rev.21.01 file

Publishers page:

Please note:

Changes made as a result of publishing processes such as copy-editing, formatting and page numbers may not be reflected in this version. For the definitive version of this publication, please refer to the published source. You are advised to consult the publisher's version if you wish to cite this paper.

This version is being made available in accordance with publisher policies.

See

<http://orca.cf.ac.uk/policies.html> for usage policies. Copyright and moral rights for publications made available in ORCA are retained by the copyright holders.



# Structural geology applied to the evaluation of hydrothermal gold deposits

T. G. BLENKINSOP<sup>1</sup>, N.H.S. OLIVER<sup>2,3</sup>, P. G. H. M. DIRKS<sup>2</sup>, M. NUGUS<sup>4</sup>, G. TRIPP<sup>5</sup>, I. SANISLAV<sup>2</sup>

*1. School of Earth and Ocean Sciences, Cardiff University CF10 3AT UK*

*2. Economic Geology Research Unit, College of Science and Engineering, James Cook University, Townsville, Queensland 4811, Australia*

*3. HCOVGlobal, Consultants, PO Box 3533, Hermit Park, Queensland 4812, Australia*

*4. AngloGold Ashanti, Strategic Technical Group, Perth, Western Australia, 6000*

*5. PO Box 42, Woodvale, Western Australia, 6026*

Corresponding Author: T. G. Blenkinsop, [BlenkinsopT@Cardiff.ac.uk](mailto:BlenkinsopT@Cardiff.ac.uk)

## Abstract

The structural geology and tectonic setting of hydrothermal gold deposits are paramount in understanding their genesis, and for their exploration. Strong structural control on mineralization is one of the defining features of these deposits, and arises because the permeabilities of crustal rocks are too low to allow the formation of hydrothermal deposits on realistic time scales unless rocks are deformed. Deformation zones and networks of deformation zones are the fundamental structures that control mineralization. Systematically analyzing deposit geometry, kinematics and dynamics leads to the most thorough comprehension of a deposit. Geometrical analysis relates ore body shape to controlling structures, and networks of deformation zones can be analyzed using topology to understand their connectivity and mineralizing potential. Kinematic analysis determines the location of permeability creation and mineralization. New views of shear zone kinematics allow for variable ratios of pure to simple shear, which change likely directions of mineralization. Multiple orientations of mineralized deformation zones may form simultaneously and symmetrically about the principal strain axes. Dynamic analysis is necessary for a mechanical understanding of deformation, fluid flow and mineralization, and can be achieved through numerical modeling. The relationship between deformation (kinematics) and stress (dynamics) constitutes the rheology: rheological contrasts are critical for the localization of many deposits. Numerous gold deposits, especially the largest, have evidence for multiple mineralizing events that may be separated by tens to hundreds of millions of years. In these cases, reactivation of structures is common, and a range of orientations of pre-existing structures are predicted to be reactivated, given that they are weaker than intact rock. Physical and chemical processes of mineralization can be integrated using a non-equilibrium thermodynamics approach.

Hydrothermal gold deposits form in contractional, strike-slip and extensional tectonic settings. However there may be great variation in the spatial scale over which the tectonic setting applies, and tectonic settings may also change on rapid time scales, so that it is inadvisable to infer local tectonics from deposit-scale patterns, and visa versa. It is essential to place mineralizing events within a complete geological history in order to distinguish pre- and post- mineralizing structures from syn-mineralization deformation features.

## Introduction

Structures have been widely recognized as one of the most important controls on hydrothermal gold deposits (Colvine, 1989; Groves and Phillips, 1987; Gustafson, 1989; Robert et al., 1995; Stillwell, 1918; Vearncombe, 1998), and they are commonly regarded as fundamental to exploration (e.g. Weinberg et al., 2004). Nevertheless, some publications on these deposits underemphasize or ignore the role of structures, and lack the detailed mapping that reveals the importance of structure, while in others it becomes a rather exclusive focus. Studies which integrate structural geology with petrography, geochemistry, and geochronology offer the greatest potential insights into ore genesis (e.g. Craw et al., 1999; Kolb et al., 2000; Bateman and Hagemann, 2004; Oliver et al., 2015). A dissenting view of the role of structural geology in gold exploration is offered by Vearncombe and Zelic (2015), who, while advocating the primacy of structural controls, argue that none of 10 structural geology paradigms in the last 60 years have lead to the discovery of gold deposits. These varying perspectives make an interesting context in which to review the role of structures in the formation of hydrothermal gold deposits. Many excellent papers address fluid flow, structures and gold deposits (e.g. Groves and Phillips, 1987; Sibson et al., 1988a; Witt and Vanderhor, 1998; Cox, 1999a), but there does not appear to be a review paper that links geometry, strain, stress and rheology to structural controls on gold mineralization.

Tectonic controls on hydrothermal deposits are also perceived to have profound and commonly simple exploration implications (e.g. Czarnota et al., 2010), such as that gold deposits are associated with particular tectonic regimes or tectonic events. Tectonics is generally considered on a larger scale than structural analysis, which raises important questions about the scales of spatial and temporal variability in tectonic regimes in relationship to tectonic controls on gold mineralization.

The aim of this review is to demonstrate how principles of structural geology can be applied to understanding hydrothermal gold deposits, including some new concepts in structural geology that may be important, although they are not yet widely tested. The question of which spatial and temporal scales are most relevant to the mineralizing processes is discussed through some case studies. An outcome of the earlier parts of the paper is a workflow for applying structural geology to gold deposits. Although some aspects of the review apply to epithermal and Carlin type gold deposits, the emphasis is strongly on lode gold deposits (including associated disseminated deposits; Bierlein and Maher, 2001), which have been commonly described as mesothermal and orogenic (Groves et al., 1998). Intrusion-related gold deposits are not explicitly considered, even

1 though they may have strong structural controls (Stephens et al., 2004). The deposits described  
2 here are bedrock gold deposits (Poulsen et al., 2000), and also “gold-only” deposits (Phillips and  
3 Powell, 2015). Problems with classification of gold deposits are considered by Poulsen (1996) and  
4 Groves et al. (1998), but are not addressed here.  
5  
6  
7  
8  
9

## 10 **Why structural geology is so important for gold deposits: Crustal** 11 **permeability, fluid flow and deformation** 12 13 14

15 Permeability, the material property that links fluid flow to differences in fluid pressure, is central to  
16 understanding the structural geology of hydrothermal ore bodies. Permeability in the crust is  
17 spatially and temporally heterogeneous and anisotropic (Farrell et al., 2014; Ingebritsen and  
18 Manning, 2010). In addition to these inherent problems of characterizing permeability, there are  
19 many ways to estimate this property, which give different results: e.g. from the record of  
20 geochemical reactions (Dipple and Ferry, 1992), by laboratory measurements (e.g. Brace, 1980), in-  
21 situ measurements, and by natural and induced seismic effects. Each of these determinations  
22 assesses permeability on different time and spatial scales, in approximately increasing order of  
23 scale. Laboratory measurements on cm scale samples are clearly unrepresentative of bulk crustal  
24 rock: this discrepancy between lab and in situ measurements is well summarized in Townend and  
25 Zoback (2000), who demonstrate that the latter are at least two to three orders of magnitude greater.  
26 Determination of the confining pressure effect on permeability has been hampered until recently by  
27 experimental procedures (Mitchell and Faulkner, 2008).  
28  
29  
30  
31  
32  
33  
34  
35  
36  
37  
38  
39  
40  
41

42 Ingebritsen and Manning (2010) therefore distinguish between mean permeability measurements of  
43 continental crust, and measurements of elevated, transient crustal permeabilities. The former can be  
44 approximated by the Manning and Ingebritsen (1999) empirical calibration of permeability ( $k$ ,  $m^2$ )  
45 with depth ( $z$ , km), which seems to hold up quite well in comparison to a variety of in situ  
46 determinations (Townend and Zoback, 2000):  
47  
48  
49  
50  
51  
52  
53

$$54 \log k = - 3.2 \log z - 14$$

55  
56  
57

58 This equation gives typical permeabilities on the order of  $10^{-16}$  to  $10^{-18}$   $m^2$  for metamorphic rocks in  
59 mid to upper crustal conditions (5 – 20 km depth) in which many hydrothermal gold deposits  
60  
61  
62  
63  
64  
65

1  
2  
3  
4  
5  
6  
7  
8  
9  
10  
11  
12  
13  
14  
15  
16  
17  
18  
19  
20  
21  
22  
23  
24  
25  
26  
27  
28  
29  
30  
31  
32  
33  
34  
35  
36  
37  
38  
39  
40  
41  
42  
43  
44  
45  
46  
47  
48  
49  
50  
51  
52  
53  
54  
55  
56  
57  
58  
59  
60  
61  
62  
63  
64  
65

formed. A lower value of  $10^{-19} \text{ m}^2$  is calculated from metamorphic reactions (Yardley, 1986). Below 15 km  $k = 10^{-18.3} \text{ m}^2$  is a good fit to the data (Ingebritsen and Manning, 2010). With this value, D'Arcy flow of sufficient volume of fluid to form a 10 Moz gold deposit through intact rocks would require 20 to 200 Ma for fluid pressure gradients of 10 to 100 MPa/km (given by the difference between lithostatic and hydrostatic pressures at depths of 5 – 20 km) (see also Cox, 1999b).

Transient crustal permeabilities may be estimated (Ingebritsen and Manning, 2010) as:

$$\log k = -3.2 \log z - 11.5$$

Below 10 km, transient permeability can be approximated as  $10^{-16} \text{ m}^2$ . If these values of transient permeability could be maintained, only 0.9 to 9 Ma would be required to form a 10 Moz gold deposit. A more sophisticated analysis that takes into account time-dependent healing after earthquake-generated permeabilities of  $10^{-13} \text{ m}^2$  suggests that such a gold deposit could form within hundreds of thousands of years (Micklethwaite et al., 2015).

Continuous fluid flow over hundreds or even tens of Ma is probably unrealistic for the formation of even large gold deposits. The above calculations and permeability requirements emphasize why hydrothermal gold deposits require deformation for their formation, and why they are so strongly controlled by structures such as fault and shear zones (e.g. Sibson, 1987; Hodgson, 1989; Poulsen and Robert, 1989; Robert et al., 1995; Cox, 1999b). Permeability may also be created by metamorphic reactions, but these are unlikely to be significant for the formation of ore bodies (Yardley and Cleverley, 2013), although metamorphic fluids have been considered as one of the key transporting agents for gold (Phillips and Groves, 1983; Phillips and Powell, 2015; Pitcairn et al., 2006). “Mobile hydrofractures”, fluid-filled fractures that propagate at  $\text{ms}^{-1}$  by opening at their upper tip and simultaneously closing at their lower tip (Bons, 2001; Oliver and Bons, 2001), may be another way in which fluids can be transferred rapidly through the crust; these too will have structural controls.

Experimental work suggests limitations on the types of deformation-induced permeability required to form gold deposits. Despite pre-failure increases in permeability of two orders of magnitude, in

1 granites at least permeability is still very low when laboratory samples are loaded up to sample  
2 failure (Mitchell and Faulkner, 2008). Even after failure, permeability along fault planes is still not  
3 greater than crustal values. These two observations imply that pervasive microcracking may not be  
4 adequate to explain permeability requirements for making an ore body, and hence larger scale  
5 structures are required. The experiments also indicate the important role of cyclic loading in  
6 building up permeability. There is some consistency between these experiments and the damage  
7 mechanics models of Sheldon and Micklethwaite (2007). These authors suggest that gold  
8 mineralization is hosted on small-displacement structures around jogs in major faults.  
9

10  
11  
12  
13  
14  
15 While transient, deformation controlled permeability is critical to forming an ore body, comparable  
16 issues need to be investigated about alteration patterns, which are typically on a larger scale than the  
17 ore bodies, but also reflect fluid-rock interactions.  
18  
19  
20  
21  
22  
23

## 24 **Applying a Classic Structural Geology Approach to Gold Deposits**

25  
26 A classical approach to structural geology distinguishes 1) geometric description (types,  
27 dimensions, orientations, and spacing of structures, and of ore bodies), 2) kinematic inference  
28 (displacements, displacement fields and strain) and 3) dynamic analysis (stress), and relates  
29 kinematic analysis to dynamics in 4) a rheological analysis (e.g. Tikoff et al., 2013). Successful  
30 progression through all four stages would achieve complete mechanical understanding of a  
31 problem, but the sequence becomes increasingly difficult to achieve as it is followed through. In the  
32 context of ore deposits, kinematic analysis is commonly limited to understanding deformation zone  
33 displacements. Dynamic analysis has concentrated on fault-controlled mineralization (e.g. Sibson et  
34 al., 1988b), and has otherwise been the preserve of the numerical modeling community (e.g.  
35 Mclellan et al., 2007). It is argued below that all three stages are potentially important for  
36 understanding ore genesis and for exploration.  
37  
38  
39  
40  
41  
42  
43  
44  
45  
46  
47  
48  
49  
50

## 51 **Geometry**

52  
53 The geometry of structurally controlled ore bodies can be approximated as planar (related to  
54 unconformities, lithological contacts, fractures, veins, deformation zones, fold hinge surfaces) or  
55 linear (related to deformation zone bends, stepovers, or intersections, fold hinges, boudin necks) at  
56 some scale (Fig. 1). The geometry of planar deformation structures that control gold mineralization  
57 can be conveniently divided into those of individual features (fractures/faults, veins, stylolites,  
58  
59  
60  
61  
62  
63  
64  
65

foliations), deformation zones, and groups of deformation zones, or networks (Fig. 2). All of these structures are associated with strain localization at some scale.

**Deformation Zones.** The description of the deformation zones is a terminological morass. Some of the most problematic issues in describing gold-associated structures are the common use of the words “brittle” and “ductile”, and the definitions and differences between faults, fault zones and shear zones. Imprecision in the use of these words leads not only to confusion but also to fundamental misunderstandings about the relationships of structures to gold mineralization. Figure 3 shows some deformation zones that are associated with gold deposits, and illustrates some of the problems.

“Brittle” and “Ductile” are highly problematic descriptors for several reasons. They have been and still are in use in at least five different ways (Tikoff et al., 2013):

1. In experimental rock mechanics, brittle behavior is contrasted with ductility, defined as a material’s ability to withstand more than 5% permanent strain before failure (Heard, 1960).
2. To distinguish deformation mechanisms e.g. brittle meaning little lattice distortion accompanying fracture (Lawn, 1993) or cataclasis compared to ductile mechanisms such as intracrystalline slip, diffusive mass transfer, or dislocation creep.
3. To distinguish crustal or lithospheric-scale rheology e.g. brittle upper crust, ductile lower crust. The “brittle –ductile” transition separates these rheological domains, and is commonly associated with hydrothermal gold mineralization (e.g. Groves et al., 2003).
4. To distinguish between brittle material that has lost cohesion and ductile material that has not (e.g. Van der Pluijm and Marshak, 2004).
5. To distinguish variations in the displacement field: Brittle deformation meaning discontinuities in the displacement field (e.g. faults) and ductile behavior meaning a progressive change in displacement field (e.g. Twiss and Moores, 2007)).

Definitions 4 and 5 are potentially useful for describing naturally deformed rocks in outcrop. However, “cohesion” is a term that has no ready objective and universal definition, and displacement fields may be hard to define, both factors leading to vagueness in applying these definitions. Another major problem that is hardly ever addressed when brittle and ductile are applied in the field is that they are scale-sensitive (Rutter, 1986). It is common to observe a macroscopically continuous (“ductile”) structure such as a fold that has formed from smaller-scale discontinuities (microfractures, stylolites). Because of the confusion introduced by the different



1 meanings of the terms brittle and ductile, their lack of precision, and their scale sensitivity, they are  
2 not useful for characterizing hydrothermal mineralization. For example, referring to a group of  
3 structures on a mine as “the brittle structures” is potentially an important confusion. Which  
4 structures would this include, and how are they relevant to the structural controls on an ore body?  
5  
6  
7

8 Even at a single scale, the type of features shown in Fig. 3C, D pose major terminological problems.  
9 These deformation zones have features that are clearly discontinuous at the scale shown, such as  
10 faults, and others, such as foliations and folded veins that are continuous at this scale. Such  
11 deformation zones are common in mesothermal gold deposits (e.g. Tripp and Vearncombe, 2004;  
12 Tunks et al., 2004). They are sometimes referred to as “brittle-ductile shear zones” or “ductile  
13 faults”. They commonly have planar, sharp boundaries, outside of which there are zones of  
14 alteration up to the width of the deformation zones, which are typically centimeters to meters wide.  
15 Within the deformation zones, there is a spectrum from planar to strongly folded veins, which may  
16 have en-echelon geometries (Laing, 2004). SC and SC’ fabrics are common, even in zones that have  
17 formed at lower greenschist facies conditions (“cataclastic SC fabrics”: Lin, 2001a). Faults are  
18 identifiable as slickensided and slickenlined surfaces. There may be porphyroclasts showing typical  
19 sigma or delta geometries. Crosscutting relationships and several generations of lineations on single  
20 surfaces show that there has been a history of multiple events, involving fabric formation, faulting  
21 and veining.  
22  
23  
24  
25  
26  
27  
28  
29  
30  
31  
32  
33  
34  
35  
36

37 Precision in geometrical description can be achieved by concentrating on continuity and specifying  
38 scale. Shear zones can be distinguished from fault zones by continuity at a given scale, and  
39 deformation zones that combine continuous and discontinuous deformation at a given scale are  
40 logically called “fault-shear zones”. It is important to note that this definition and Fig. 2 are not  
41 simply a replacement for the terms brittle and ductile. Continuity, specified at a given scale, is a  
42 precise and unambiguous way to describe ore-hosting structures. It is recommended to avoid the use  
43 of the terms brittle and ductile: there are several more precise alternatives depending on the context.  
44 Some of these alternatives are given above in the analysis of meanings for brittle and ductile: for  
45 example, in the context of deformation mechanisms, terminology such as fracture, cataclasis  
46 dislocation creep, diffusion creep or diffusive mass transfer can be used.  
47  
48  
49  
50  
51  
52  
53  
54  
55  
56  
57

58 ***Ore Body Geometry.*** The geometry of ore bodies needs to be understood in order to relate them to  
59 the structures and processes that control them. Hydrothermal ore bodies may have very complex  
60  
61  
62  
63  
64  
65

1 shapes in detail, but many can be simplified into an ellipsoid with maximum (U), intermediate (V)  
2 and minimum (W) axes (Blenkinsop, 2004a). By analogy with the strain ellipsoid, it is possible to  
3 define the shape of the ore body by the parameter  $j = (U/V - 1)/(V/W - 1)$  which divides ore bodies  
4 into prolate ( $j > 1$ ) and oblate ( $j < 1$ ) shapes, and to specify the orientation of the ore body through the  
5 trend and plunge of the U and W axes. These descriptions can also be used to understand the  
6 evolution of the ore bodies, for example by studying how  $j$  may change with growth inferred from  
7 ore body size (Blenkinsop 2004a); however, since ore body shapes may be influenced by pre-  
8 mineralization geometry, and syn- and post-mineralization deformation events, it is important to  
9 relate ore body geometry to the whole structural history.  
10  
11  
12  
13  
14  
15  
16  
17

18 **Network Topology.** Structural complexity and density of fractures is recognized as important in  
19 controlling gold mineralization potential (e.g. Tripp and Vearncombe, 2004). More specifically, the  
20 geometry of networks of deformation zones controls ore bodies on scales larger than the individual  
21 deformation zones. Network geometry is usually described by attributing the component  
22 orientations into sets, and measuring the spacing, frequency, density or intensity of traces of  
23 deformation zones (Dirks et al., 2013; Riley, 2005). However, traces can be ambiguous to interpret  
24 where there is splaying. For example, at the intersection of the three branches indicated by “?” on  
25 Fig. 4, a vein trace splits and it is unclear which branch belong to the same unique trace. Traces are  
26 subject to a greater amount of sampling bias (censoring) (Sanderson and Nixon, 2015), and trace  
27 analysis does not capture the topology of networks, which is critical for measuring connectivity.  
28 Topological analysis of networks focuses on branches, defined as segments of a trace between  
29 nodes, where the trace either terminates, or joins two or three other branches (Fig. 4). These  
30 locations are I, Y and X nodes respectively, and the proportions of each type of node characterize  
31 the network topology. The average number of connections per branch ( $C_B$ ) partly characterizes  
32 network connectivity (Sanderson and Nixon, 2015). Since each Y node connects to 3 branches, and  
33 each X node to 4,  
34  
35  
36  
37  
38  
39  
40  
41  
42  
43  
44  
45  
46  
47  
48  
49

$$50 \quad C_B = (3N_Y + 4N_X) / N_B$$

51  
52  
53  
54  
55 Where  $N_Y$ ,  $N_X$ , and  $N_B$  are the number of X and Y nodes and branches respectively. Thus in Fig. 4.  
56  $C_B = (30 + 12) / 28 = 1.5$ . This number seems to be typical of a number of natural fracture networks.  
57  
58 Topological measures such as  $C_B$  are independent of any scale.  
59  
60  
61  
62  
63  
64  
65

1  
2  
3  
4  
5  
6  
7  
8  
9  
10  
11  
12  
13  
14  
15  
16  
17  
18  
19  
20  
21  
22  
23  
24  
25  
26  
27  
28  
29  
30  
31  
32  
33  
34  
35  
36  
37  
38  
39  
40  
41  
42  
43  
44  
45  
46  
47  
48  
49  
50  
51  
52  
53  
54  
55  
56  
57  
58  
59  
60  
61  
62  
63  
64  
65

However, the permeability of a network will depend not only on relative numbers of different types of nodes, but also the intensity of the branches, as assessed by their number or length per unit area or area per unit volume. Both connectivity and intensity can be measured from branch analysis, and can be combined to characterize the likely permeability properties of the network (Sanderson and Nixon, 2015). This type of analysis, developed in three dimensions, would seem highly suited to evaluating the resource potential of stockworks. Network analysis is closely aligned to percolation theory (Stauffer and Aharony, 1994), which has interesting potential for understanding hydrothermal mineralization (Blenkinsop, 2014). Networks are also useful to describe 3D model topologies (Thiele et al., 2016a, 2016b).

18  
19  
20  
21  
22  
23  
24  
25  
26  
27  
28  
29  
30  
31  
32  
33  
34  
35  
36  
37  
38  
39  
40  
41  
42  
43  
44  
45  
46  
47  
48  
49  
50  
51  
52  
53  
54  
55  
56  
57  
58  
59  
60  
61  
62  
63  
64  
65

Network topology may also be one way to probe an enigma posed by the relationship between hydrothermal gold deposits and first and lower “order” structures. A common view is that gold deposits are hosted in lower (second, third etc.) order structures adjacent to, but not on, first order (major) structures (Eisenlohr et al., 1989; Blenkinsop et al., 2000; Weinberg et al., 2004). Lower order structures correspond to dangling elements in a network (Cox, 1999). In the above terminology, these are branches that join I to Y or X nodes. The location of gold deposits on lower order structures is attributed to the greater opportunities for fluid-rock interaction or fluid mixing afforded by these structures. However, there are several examples where the largest regional structures do host important gold deposits, including the Ashanti deposit at Obuasi (Blenkinsop et al., 1994; Allibone et al., 2002a) and deposits at Bogoso (Allibone et al., 2002b), both in Ghana, and Kerr Addison, Kirkland Lake, Canada (Jia and Kerrich, 2000). Considering the deformation zones as networks and analyzing the branch geometry would be an effective way to test the relationship of deposits to structural hierarchy, and to determine if there is indeed a general pattern. An important consideration for implementing network analysis is to demonstrate that the analyzed deformation zones were simultaneously active, and that the pattern is not a product of overprinting or selective reactivation of older structures or lithostratigraphic contacts.

## Kinematics

54  
55  
56  
57  
58  
59  
60  
61  
62  
63  
64  
65

The kinematics of deformation zones and networks during mineralization, in combination with their geometry, determine sites of deformation-enhanced permeability. Dilational stepovers (jogs) and bends in deformation zones (e.g. Weinberg et al., 2004) are commonly regarded as particularly favorable for mineralization, but fracturing and permeability are also created at contractional stepovers and bends (e.g. Ford et al., 2009). Deformation zone roughness or non-planarity can

1 therefore be an important aspect of prospectivity. Deformation zones represent crustal weaknesses  
2 that may be reactivated many times. Distinguishing between pre-, syn- and post-mineralization  
3 kinematics is therefore important, especially when mineralization has occurred in repeated events or  
4 gold has been remobilized. Mineralization needs to be placed in a complete kinematic history by  
5 analysis of relative age via overprinting relationships and timing compared to geological events  
6 such as intrusions (e.g. Miller and Wilson, 2004), and by absolute age dating (e.g. Morelli et al.,  
7 2010). A rigorous application of structural geology to understanding hydrothermal mineral deposits  
8 results in terminology ( $D_1, D_2, D_n, S_1, S_2, S_n, L_1, L_2, L_n$  etc. e.g. Table 1) that can appear to verge on  
9 jargon to the non-specialist, but in many cases this notation is an efficient if not essential way to  
10 present a complex spatio-temporal sequence in an orderly fashion. New understanding of the  
11 kinematics of individual deformation zones, and their networks, has special significance for  
12 interpreting syn-kinematic mineralization as described below.  
13  
14  
15  
16  
17  
18  
19  
20  
21  
22

23 **General Shear.** A new perception about the kinematics of individual shear zones has developed  
24 over the last 25 years, which focuses attention on relationships between the foliation, shear plane,  
25 shear direction, direction of maximum elongation (lineation), and the vorticity vector. The vorticity  
26 vector in particular is a key concept, which can be thought of informally as the “rolling axis” in  
27 shear (Fig. 5). Previously the paradigm for shear zones was based on the Ramsay and Graham  
28 (1970) model that shear zones were localized zones of inhomogeneous simple shear, in which the  
29 lineation and shear direction are perpendicular to the vorticity vector. However, observations and  
30 models of shear zones where the lineation is parallel to the vorticity vector contradict the  
31 perpendicular relationship predicted by the Ramsay and Graham model, and these situations have  
32 instead been explained by models with significant components of pure shear (Fig. 5, e.g. Tikoff and  
33 Fossen, 1993; Fossen, 1993; Tikoff and Greene, 1997; Tikoff and Fossen, 1999). Many of these  
34 models were framed in the context of transpression (Sanderson and Marchini, 1984; Jones and  
35 Holdsworth, 1998; Lin et al., 1998). Possibilities of even more variable relationships among  
36 foliation, lineation, shear direction and the vorticity vector have resulted from further work,  
37 including those of triclinic shear (Jiang and Williams, 1998; Lin et al., 1998). These advances have  
38 yet to be fully incorporated into studies of mineralized shear zones (but see Lin, 2001b), so that it is  
39 unclear how widely general shear has affected gold deposits, but the following examples  
40 demonstrate that where a new appreciation of shear zone kinematics has been applied, it has had  
41 profound consequences for understanding syn-mineralization deformation.  
42  
43  
44  
45  
46  
47  
48  
49  
50  
51  
52  
53  
54  
55  
56  
57  
58  
59  
60

61 The importance of pure shear components is illustrated by the Taurus shear zone at Golden Pig  
62  
63  
64  
65

1 mine, Southern Cross Greenstone belt, Yilgarn craton (Nugus et al., 2003). The Taurus Lode at  
2 Golden Pig is hosted by an intensely deformed sequence of predominantly mafic and ultramafic  
3 rocks with intercalated Banded Iron Formations (BIF) and sedimentary rocks. The Taurus shear  
4 zone comprises a zone of steeply WSW dipping schistosity (S) with a strong biotite, amphibole and  
5 pyrrhotite lineation (L) plunging 10° S. Underground exposures show the kinematics of the shear  
6 zone very clearly. On drive headings, perpendicular to the foliation and lineation, there is consistent  
7 evidence for reverse shear, while roof views parallel to the lineation and perpendicular to the  
8 foliation show sinistral and dextral asymmetries, from deformed veins. The vorticity vector appears  
9 to be parallel to the lineation, suggesting a pure-shear dominated shear zone, with a reverse  
10 component (Fig. 6). The large amount of flattening may be related to the position of the shear zone  
11 between two adjacent granite domes. Ore body long axes (*U* axes) plunge parallel to the lineation  
12 and vorticity vector (Nugus et al., 2003).  
13  
14  
15  
16  
17  
18  
19  
20  
21  
22

23 Another example where pure shear may be dominant is part of the Arcturus deposit in the Shamva  
24 greenstone belt, Zimbabwe. The pyrrhotite-arsenopyrite-pyrite ore bodies are hosted in a network of  
25 shear zones up to 1 km wide, defined by S – L fabrics of biotite-actinolite-quartz-epidote-fuchsite  
26 (Mutemeri, 2001). Shear zones dip steeply to the N or NE, and ore body *U* axes and lineations also  
27 plunge in this direction in the Ceylon section of this mine (Fig. 7). However, dextral asymmetries  
28 are seen in plan view, suggesting a vorticity vector plunging parallel to the lineation, and a  
29 dominant component of pure shear (Blenkinsop, 2004a).  
30  
31  
32  
33  
34  
35  
36  
37  
38

39 These situations contrast with mineralized shear zones dominated by simple shear, as illustrated by  
40 two more examples from Zimbabwe. In the Renco mine, Northern Marginal Zone of the Limpopo  
41 belt, the major ore bodies are hosted within four main shear zones 0.1 to 3 m wide dipping gently to  
42 the southeast (Blenkinsop and Frei, 1996). Shear zones consist of quartz-feldspar-biotite-  
43 hornblende mylonites and garnet-biotite-feldspar-quartz tabular pods where pyrrhotite, chalcopyrite  
44 and pyrite are associated with mainly free gold (Kisters et al., 2000; Kolb et al., 2000). Mineral  
45 stretching lineations plunge down dip (Fig. 7). Clear shear sense indicators are seen on planes  
46 parallel to the lineation and perpendicular to the foliation, giving a reverse sense of shear in the  
47 north part of the mine (Kisters et al., 1998). The *U* axes of ore bodies plunge generally to the  
48 southeast (Blenkinsop and Kadzviti, 2006), parallel to the lineations and perpendicular to the  
49 inferred vorticity vector (Fig. 7). These kinematics are compatible with the observed thrust sense of  
50 movement of the Northern Marginal Zone over the Zimbabwe craton, which occurred at the end of  
51 the Neoproterozoic (Blenkinsop et al., 2004), and with simple-shear dominated kinematics. The oblate  
52  
53  
54  
55  
56  
57  
58  
59  
60  
61  
62  
63  
64  
65

1 shapes of these ore bodies, and their orientation parallel to the lineation, can be explained by higher  
2 permeabilities within the shear zone and parallel to the shear direction. Variations in the ore body  
3 orientation may reflect a process of ore body growth by coalescence (Blenkinsop and Kadzviti,  
4 2006).  
5  
6  
7

8 The Shamva mine in the Harare-Shamva greenstone belt, Zimbabwe, is another example of a  
9 deformation zone hosted gold deposit with simple-shear dominated kinematics, but with a different  
10 arrangement of ore bodies and shear directions compared to the Renco case. The Shamva ore  
11 bodies are hosted in the sub-vertical NE-trending Shamva shear zone, which has a sinistral strike-  
12 slip sense of shear (Jelsma et al., 1998). The shear zone consists of a network of principal (Y) and  
13 Riedel (R) shears, which intersect in steeply plunging lines, and show a typical strike-slip  
14 configuration. The *U* axes of the pyrite-carbonate ore bodies with an alteration assemblage of  
15 biotite-tourmaline-oxide-carbonate-quartz plunge steeply, perpendicular to sub-horizontal  
16 slickenfibres lineations (Blenkinsop, 2004a). The ore bodies formed along shears in R and Y shear  
17 orientations, and at their intersections. In this case the ore bodies are parallel to the vorticity vector  
18 and perpendicular to the lineation, in contrast to the situation at Renco, where ore bodies are parallel  
19 to the lineation but perpendicular to the vorticity vector.  
20  
21  
22  
23  
24  
25  
26  
27  
28  
29  
30  
31  
32

33 The three studies illustrate three different types of kinematic control through three possible relations  
34 among ore bodies, lineations and vorticity vectors (Figs. 5, 7). In the pure shear dominated cases of  
35 Golden Pig and the Ceylon section of the Arcturus deposit, ore body *U* axes form parallel to the  
36 lineation and the vorticity vector. In the simple shear dominated cases of Renco and Shamva, there  
37 seem to be two possibilities. At Renco, ore body *U* axes are parallel to the lineations and  
38 perpendicular to the vorticity vector (Fig. 7). They formed in such an orientation because of  
39 enhanced permeability in the shear zone fabric. In contrast, at Shamva, the *U* axes are perpendicular  
40 to the lineations and parallel to the vorticity vector. The control on the ore bodies may also have  
41 been permeability, but in this case the greatest permeability was along intersections between shears,  
42 which are parallel to the vorticity vector and perpendicular to the lineations (Fig. 5C, 7C).  
43  
44  
45  
46  
47  
48  
49  
50  
51  
52  
53

54 The relationships between ore bodies, lineations and vorticity vectors may partly be a function of  
55 metamorphic grade: there is a need for more systematic documentation of these relationships to  
56 explore this further. It is also important to note that progressive deformation can lead to  
57 overprinting relationships within the same deformation event (e.g. as material lines rotate from  
58  
59  
60  
61  
62  
63  
64  
65

1 shortening to lengthening fields), and that post-mineralization deformation may affect ore body  
2 geometry and therefore interpretations of kinematic controls on ore bodies. Additional  
3 complications in kinematic interpretations can also be expected where there have been multiple  
4 mineralizing events in the same deposit (see below).  
5  
6  
7

8 ***Conjugate and Polymodal Networks.*** Deformation zones may form conjugate or polymodal  
9 geometries that are symmetrical about bulk principal strain axes, and hence control mineralization  
10 in systematic patterns. Conjugate faults, that is two orientations symmetrically disposed at acute  
11 angles to the maximum shortening direction, dominate conceptions of how faults interact (cf.  
12 Anderson, 1905). However, such conjugate faults can only accommodate plane strain (Healy et al.,  
13 2015). Experiments (e.g. Oertel, 1965; Aydin and Reches, 1982), field observations (Woodcock and  
14 Underhill, 1987; Oesterlen and Blenkinsop, 1994; Carvell et al., 2014), and theory (Oertel, 1965;  
15 Reches, 1983), by contrast, emphasize that fault networks are polymodal, consisting of four  
16 orientations (quadrимodal) of simultaneously active faults, or a dispersion of orientations (Fig. 8).  
17 Intersections between polymodal networks of faults can have complex geometries (Healy et al.,  
18 2015). Quadrимodal patterns have also been reported for deformation bands (Underhill and  
19 Woodcock, 1987) and kink bands (Kirschner and Teixell, 1996). The formation of quadrимodal  
20 kink bands was contemporary with mineralization at Bendigo, Victoria, and these kink bands  
21 control mineralization on millimeter to kilometer scales (Raine, 2005).  
22  
23  
24  
25  
26  
27  
28  
29  
30  
31  
32  
33  
34  
35  
36

37 Shear zone networks may form in conjugate pairs (Mitra, 1979) but they also commonly have  
38 orientations that are more varied, forming networks that isolate lozenges of less-deformed rock,  
39 which approximate the shape of the strain ellipsoid (Fig. 8: Choukroune and Gapais, 1983; Gapais  
40 et al., 1987; Kruckenberg et al., 2010). These patterns can accommodate general shear (Hudleston,  
41 1999). Quadrимodal shear zone networks were demonstrated to control ore bodies at the very high  
42 gold grade Norbeau deposit, Quebec (Dube et al., 1989). Here, quartz veins occur in four sets of  
43 shear zones within a metamorphosed layered mafic intrusion. The shear zones are compatible with a  
44 single strain field, which consists of down-dip extension of the sill and strike-parallel shortening.  
45 The orientation of the sill appears to have guided the principal strains because of its competence.  
46  
47  
48  
49  
50  
51  
52  
53  
54  
55

56 Polymodal patterns of deformation zones have major implications for understanding of the basic  
57 principles of deformation and for ore body geometry. Since polymodal faults and shear zones have  
58 clear relationships to strain ellipsoids and non-plane strain, it is evident that kinematics are  
59  
60  
61  
62  
63  
64  
65

1  
2  
3  
4  
5  
6  
7  
8  
9  
10  
11  
12  
13  
14  
15  
16  
17  
18  
19  
20  
21  
22  
23  
24  
25  
26  
27  
28  
29  
30  
31  
32  
33  
34  
35  
36  
37  
38  
39  
40  
41  
42  
43  
44  
45  
46  
47  
48  
49  
50  
51  
52  
53  
54  
55  
56  
57  
58  
59  
60  
61  
62  
63  
64  
65

fundamental to both faulting and shearing, including deformation bands and kink bands (cf. Marrett and Allmendinger, 1990; Hudleston, 1999; Healy et al., 2015 ). The patterns of deformation zones shown in Fig. 8 are similar in: i) having an orthorhombic symmetry about the bulk principal strain axes and ii) having four clusters (or orientations distributed around four modes). These similarities argue for a kinematic “control” on deformation zones. The bulk strain patterns accommodate non-plane strain (Healy et al., 2015), and, at least for faults, form in true triaxial stress conditions (Chang and Haimson, 2012), which are likely to be common in the crust (Lisle et al., 2006).

Polymodal patterns of deformation zone networks may be more widespread than generally appreciated, for the reasons suggested in Healy et al. (2015). Because the recognition of the generality of polymodal patterns is recent, their implications for ore bodies are not widely known, but at least in some cases it is evident that ore bodies may form along the four orientations of the deformation zones (Raine, 2005; Dube et al., 1989). One may also predict that shoots may be localized along the four directions of intersections of polymodal deformation zones because they are directions of enhanced permeability.

## Dynamics

It is difficult to overemphasize the importance of the fault valve model ( Sibson et al., 1988) for the insights that it has brought to the dynamic understanding of gold mineralization. Four major perceptions that come from this model are:

- 1) Transient permeability for large fluid fluxes is created by movement on deformation zones. This has obvious exploration implications: geometries of favorable deformation zones may combine continuous and discontinuous deformation, as commonly observed (e.g. Robert et al., 1995).
- 2) Reactivation and repeated deformation characterize the formation of ore bodies. This point has important implications for deciphering structural histories, in which changes in kinematics and stresses during a mineralizing event should not be mistaken for longer-term distinct orogenic episodes.
- 3) Fluid pressure fluctuations, perhaps associated with the seismic cycle and involving supralithostatic pressures, are critical. This point suggests that unfavorably orientated structures, requiring high fluid pressures for reactivation, may be preferred structures for ore bodies.



- 1  
2  
3  
4  
5  
6  
7  
8  
9  
10  
11  
12  
13  
14  
15  
16  
17  
18  
19  
20  
21  
22  
23  
24  
25  
26  
27  
28  
29  
30  
31  
32  
33  
34  
35  
36  
37  
38  
39  
40  
41  
42  
43  
44  
45  
46  
47  
48  
49  
50  
51  
52  
53  
54  
55  
56  
57  
58  
59  
60  
61  
62  
63  
64  
65
- 4) Fluid pressure decrease leads to gold precipitation. This mechanism may explain contrasting styles of ore bodies in the same deposit. Vein hosted gold may form by pressure decrease, while replacement ore may form from fluid-rock interaction.

The link established by the fault valve model between gold mineralization and the seismic cycle leads naturally to the application of Coulomb stress, or stress transfer, modeling (Cox and Ruming, 2004). This type of modeling simulates the static stress changes that would be associated with seismic movement of a given fault geometry. Application to the St Ives gold field, Yilgarn craton shows how the location of gold mineralization corresponds to the predicted position of aftershocks from a main shock rupture on the adjacent Bolder-Lefroy fault system (Micklethwaite and Cox, 2004; 2006). The aftershocks created zones of high permeability. An attractive aspect of this hypothesis is that it explains the common observation that mineralized structures for lode gold style deposits in particular have low displacements, and occur adjacent to major structures. It is important to establish that all faults included in the model were active at the time of mineralization.

Finite element modeling (FEM) has also proven of value in understanding hydrothermal gold deposits (Holyland and Ojala, 1997; Schaub et al., 2006; Schaub and Zhao, 2002). McLellan et al. (2007) show how structural analysis can be used to infer stress conditions leading to failure on shear zones. Applying these stress conditions leads to predictions of volumes of high shear strain, dilation and most likely failure, which have important exploration applications. An important part of the modeling is to include the effect of the stress ratio,  $\Phi = (\sigma_2 - \sigma_3)/(\sigma_1 - \sigma_3)$  (Angelier, 1975), which varies from 0 for  $\sigma_2 = \sigma_3$ , to 1 for  $\sigma_1 = \sigma_2$ . Table 1 shows how variable  $\Phi$  values were used during the tectonic history at Sunrise Dam; taking this into account made a significant difference to the modeling results. Another illustration of the importance of dynamic analysis comes from the Magdala gold deposit, in the Lachlan fold belt, Victoria (Miller and Wilson, 2004a). By reconstructing the stress history from fault slip measurements, the existence of a displaced footwall ore body (the Golden Gift ore body) was predicted, based on the position of the hanging wall Magdala ore body that was being mined. It was possible to establish a detailed stress history; again, the stress ratio  $\Phi$  had significant effects, in this case on predicted fault slip directions. However, application of FEM models becomes considerably more complex, and less predictive, when the effects of varying strain rates, heating, chemical reaction and permeability are considered, and when 2D modeling is applied to 3D situations.

1  
2  
3  
4  
5  
6  
7  
8  
9  
10  
11  
12  
13  
14  
15  
16  
17  
18  
19  
20  
21  
22  
23  
24  
25  
26  
27  
28  
29  
30  
31  
It is puzzling that Coulomb stress modeling and FEM both appear to be successful, since the first considers only stress changes caused by increments of slip, and the second uses a constant remote applied stress and does not take into account changes in stress due to discrete slip events. This paradox leads to an important uncertainty about mechanical models for hydrothermal gold deposits. Faults have been regarded as either slipping seismically (Coulomb stress modeling) or creeping aseismically (FEM), but recently it has become clear that there is a spectrum of fault slip modes that include seismic slip, episodic tremor and slip, slow earthquakes, and fault creep (e.g. Ben-zion, 2008; Gomberg, 2010; Beroza and Ide, 2011). Although many of the relevant observations come from the Cascadia and Nankai subduction zones, similar phenomena are now recognized on normal faults in rifts (Calais et al., 2008), and in the San Andreas fault and other strike-slip and oblique slip fault systems (Chamberlain et al., 2014; Jolivet et al., 2014). Continuous, aseismic sliding (creep) has now been observed, thanks to more extensive geodetic coverage, on a variety of types of faults around the world, at speeds up to those of plate motions ( $10^{-9}$  ms<sup>-1</sup>). Observations of fault slip between the extremes of seismic and continuous aseismic modes have collectively been termed slow-slip phenomena, and are recognized as components of a continuum of fault behavior (Peng and Gomberg, 2010). The fundamental controls on the spectrum of fault slip modes and speeds are not known.

32  
33  
34  
35  
36  
37  
38  
39  
40  
41  
42  
43  
44  
45  
46  
47  
48  
49  
50  
51  
52  
53  
54  
55  
56  
57  
58  
59  
The phenomenology of slow slip makes it likely to be important in gold mineralization. Seismic signals associated with slow-slip events indicate that they are due to slip on faults, like earthquakes. It is very likely that pore fluids at high pressures are involved (e.g. Chamberlain et al., 2014). Moreover, there is field evidence to support the link between slow slip and gold mineralization. Fagereng and Sibson (2010) demonstrated that mixed continuous-discontinuous deformation zones observed in the field, comparable to fault-shear zones that host gold (e.g. Fig. 3C, D), may have the correct physical properties for different types of fault slip. Furthermore, veins with similar crack-seal textures to those seen in gold deposits (e.g. Boullier and Robert, 1992; Robert et al., 1995), have the correct geometrical properties to generate the episodic tremor that is associated with slow slip events (Fagereng et al., 2011). The possibility of slow slip as a hydrothermal gold mineralization mechanism has not been widely considered, or included in numerical models for mineralization.

## 60 61 62 63 64 65 **Rheology**

The determination of relationships between deformation and stress, “rheology” in the broadest

1 sense, is perhaps the most difficult part of a structural analysis, since about the only aspect of a  
2 complex ore deposit that can be well constrained is generally the present geometry, allowing  
3 estimates of some displacements and strain. Common methods of dynamic analysis for the reduced  
4 stress tensor are limited to discontinuous deformation; strain rates are commonly unknown, and  
5 material properties at the time of deformation can be little more than guesses. Despite these  
6 limitations, rheological explanations for mineralization are some of the most commonly invoked,  
7 perhaps because of the obvious localization of mineralization along rheological contacts or within  
8 units with distinct rheology. A good example comes from Renco gold mine, Zimbabwe, for which  
9 the kinematics were described above. Gold mineralization within mylonitic shear zones developed  
10 at mid-upper amphibolite facies is concentrated in meter-wide competent lithons consisting of an  
11 alteration assemblage of quartz, feldspar biotite and garnet which has veins, fractures, breccias and  
12 abundant sulphides, mainly pyrrhotite (Kisters et al., 2000; Kolb et al., 2000). These lithons are  
13 mineralized because they fractured, creating dilatancy, compared to the flow in the adjacent  
14 protomylonites and mylonites. Fracturing may have occurred during seismic events. A much larger  
15 scale rheological control is seen in the localization of mineralization the around the Scotia-  
16 Kanowna Dome, in the east Yilgarn craton, Australia. There, the world-class Kanowna Belle  
17 deposit was formed because mineralizing fluids were focused into a dilatant volume at the nose of  
18 the Scotia-Kanowna Dome (Davis et al., 2010a). Smaller deposits were also formed in shear zones  
19 localized around the sides of the dome. The same rheological contrasts may account for patterns of  
20 mineralization in other parts of the Yilgarn craton. Sites of low mean stress have the potential to  
21 focus fluid flow and may have negative fluid pressures, resulting in extensional veining and dilation  
22 (Ridley, 1993).  
23  
24  
25  
26  
27  
28  
29  
30  
31  
32  
33  
34  
35  
36  
37  
38  
39  
40  
41  
42

### 43 **Reactivation and Multiple Mineralizing Events**

44 It is obvious from many hydrothermal gold deposits that structures that formed in earlier tectonic  
45 events are reused by fluids and localize mineralization during a subsequent deformation/  
46 mineralization event. A clear signpost to the importance of such reactivation is syn-mineralization  
47 deformation of zones in “unfavorable” orientations i.e. orientations that have lower ratios of shear  
48 to normal stress than the optimum orientation (Fig. 9). A classic example are the high angle reverse  
49 faults in the Sigma mine, Canada, which originated as normal or strike slip faults (Sibson et al.,  
50 1988), and required supralithostatic pore fluid pressures for reactivation (Boullier and Robert,  
51 1992). Another example is provided by the St Ives goldfield, Western Australia, where a set of  
52 WNW trending faults links mineralized N-trending faults (Miller et al., 2010). The WNW trending  
53 faults correspond to isopach thickness variations and so were probably active as normal faults  
54  
55  
56  
57  
58  
59  
60  
61  
62  
63  
64  
65

1 during basin formation, 50 Ma earlier than gold mineralization. A third example comes from the  
2 Kainantu gold mine in Papua New Guinea (Blenkinsop et al., 2017). Gold-copper mineralization  
3 with classic epithermal textures occurs in NW-SE steeply dipping veins. These veins are developed  
4 along a dextral strike slip shear zone network, which itself is generally parallel an earlier  
5 greenschist facies cleavage in the host rocks. High Au grades correlate with areas of obliquity  
6 between the shear zone fabrics and the cleavage, and plunge at  $\sim 40^\circ$  southeast parallel to hinges of a  
7 crenulation cleavage. The cleavage could be as old as the Jurassic; mylonitization and crenulation  
8 may date between 40 Ma and 9 Ma, and mineralization is probably related to an extensional phase  
9 of deformation at 9 – 6 Ma. Mineralization was followed by strike-slip faulting in the same  
10 orientation as the mineralized veins that is compatible with the current N-S convergence, which has  
11 been ongoing for the last 4 – 5 Ma. The relatively recent and well-preserved geological history at  
12 Kainantu allows a detailed history of reactivation to be deciphered and related to the tectonic  
13 history. In this case reactivation of fabrics, shear zones and veins with the same orientation has  
14 occurred over as long as 200 Ma in at least 4 discrete events.  
15  
16  
17  
18  
19  
20  
21  
22  
23  
24  
25

26 A general prerequisite for reactivating faults is a reduction in either or both cohesion and coefficient  
27 of internal friction along the reactivated fault (Fig. 9), otherwise new faults will form in intact rock  
28 rather than older structures being reactivated. In all cases it is apparent that a range of orientations  
29 can be reactivated for a fault that is weaker than intact rock, in a given stress state. Reactivation  
30 may therefore be common where there are pre-existing discontinuities in a variety of orientations.  
31 For very unfavorable orientations, reactivation will require supralithostatic pressure (Sibson, 1985).  
32  
33  
34  
35  
36  
37  
38  
39

40 The reactivation potential of cohesionless faults is conveniently analyzed by the slip and dilation  
41 tendencies. Slip tendency measures the propensity for a fault to reactivate in shear, and dilation  
42 tendency is the propensity for extensional reactivation (Moeck et al., 2009; Morris et al., 1996). The  
43 tendencies can be normalized to frictional properties so that the most favorable orientation for  
44 reactivation has a tendency of 1 and the least favorable (no reactivation) has a tendency of 0 (Lisle  
45 et al., 2006; Moeck et al., 2009). An advantage of this method for analyzing reactivation is that it  
46 shows clearly how the relative value of the intermediate stress has a major effect on the pattern of  
47 expected reactivation (Morris and Ferrill, 2009) (Fig. 10). Given that the most common state of  
48 stress in the crust has  $\Phi = 0.3$  (Lisle et al., 2006), any fault at angles of 20-40° to  $\sigma_1$  has a high slip  
49 tendency, while a range of orientations of faults sub-parallel to  $\sigma_1$  have high dilation tendencies  
50 (Fig. 10).  
51  
52  
53  
54  
55  
56  
57  
58  
59  
60  
61  
62  
63  
64  
65

1 While it may seem intuitive that a pre-existing fault has lower strength, experiments indicate that  
2 crack healing and strength recovery can be rapid (on the order of hours at high temperatures) due to  
3 compaction and cementation (Smith and Evans, 1984). However, reduction in permeability also has  
4 the effect of increasing pore fluid pressures, facilitating failure (Tenthorey et al., 2003). There is  
5 therefore likely to be feedback between deformation, permeability creation, pore fluid pressure,  
6 fluid movement and cementation, possibly creating complex behavior on reactivated faults  
7 (Barnhoorn et al., 2010).  
8  
9  
10

11  
12  
13  
14 Advances in dating mineralization have made it clear that the endowment of several major gold  
15 deposits or goldfields has accumulated in distinct events separated by tens or even hundreds of  
16 millions of years. For example, Frei et al., (1998) showed that Archean gold mineralization at 2.60  
17 Ga in the Kimberly-RAN mines in Zimbabwe was followed by Early Proterozoic gold deposition at  
18 1.96 Ga. In the central Victorian goldfield, Australia, initial gold mineralization occurred in the Late  
19 Ordovician, during the early stages of the accretionary development of the Lachlan fold belt,  
20 followed by Late Devonian mineralization at 376 Ma (Arne et al., 2001). In the Meguma terrane,  
21 Nova Scotia, mineralization occurred at two times in the Devonian, 407 Ma and ca. 380 Ma  
22 (Morelli et al., 2005). These are correlated with regional Acadian orogenesis and granite  
23 intrusion/high grade metamorphism respectively. Reactivation is likely to be a key to adding extra  
24 resources in situations of multiple mineralizing events.  
25  
26  
27  
28  
29  
30  
31  
32  
33  
34  
35  
36  
37

## 38 **Thermodynamics: An integrated approach**

39  
40

41 A systems approach to hydrothermal gold mineralization has been advocated for some time (Fyfe  
42 and Kerrich, 1976; McCuaig and Hronsky, 2016; Wyborn et al., 1994) but many studies are  
43 qualitative and have focused on exploration implications rather than genetic understanding of  
44 mineralization (Wyman et al., 2016). The systems approach clarifies that the formation of an ore  
45 body involves many feedbacks and is likely to be highly non-linear (Ord et al., 2012). Non-  
46 equilibrium thermodynamic approaches to deformation (Hobbs et al., 2012) and mineralization  
47 (Ord et al., 2016, 2010) offer a chance to quantify a systems analysis and to use it to understand the  
48 fundamentals of forming an ore body (Fig. 11). The model proposed by Ord et al. (2012), Lester et  
49 al. (2011) and Hobbs and Ord (2017) treats ore body formation as an open system reactor in which  
50 a sustained flux of reactants and energy creates alteration through exothermic reactions initially,  
51 which subsequently undergo competition from endothermic ore precipitation reactions.  
52 Deformation, fluid transport, heat and chemical reactions are all coupled (Fig. 11). A prediction of  
53  
54  
55  
56  
57  
58  
59  
60  
61  
62  
63  
64  
65

1  
2  
3  
4  
5  
6  
7  
8  
9  
10  
11  
12  
13  
14  
15  
16  
17  
18  
19  
20  
21  
22  
23  
24  
25  
26  
27  
28  
29  
30  
31  
32  
33  
34  
35  
36  
37  
38  
39  
40  
41  
42  
43  
44  
45  
46  
47  
48  
49  
50  
51  
52  
53  
54  
55  
56  
57  
58  
59  
60  
61  
62  
63  
64  
65

this approach is that ore bodies are multifractal and have spatial scale invariance (Munro et al. 2017).

## **Spatial and temporal variability in tectonic controls on hydrothermal gold deposits**

Compressional and transpressional tectonic controls on gold mineralization at local and regional scales are widely documented (e.g. Groves et al., 1998; Goldfarb et al., 2001; Goldfarb et al., 2005). However, there are many examples that show how extensional and strike slip tectonic settings at a variety of scales may also be important, illustrated in the following case studies. The Shamva shear system described above has a Riedel geometry that is consistent with sinistral simple shear, and no shortening component to render it transpressional (Jelsma et al., 1998; Blenkinsop, 2004a). Sunrise Dam is one of Australia's premier gold mines, situated in the Laverton greenstone belt on the Yilgarn craton, and hosted in andesitic to basaltic volcanoclastic rocks, iron formation, turbidites and porphyry sills and dykes. In several respects Sunrise Dam Gold Mine is a typical greenstone-hosted, late Archean lode gold deposit. As usual for a world-class resource, there are several styles of mineralization and important variations through the mine among shear zone-, stockwork-, breccia- and vein-hosted mineralization. The rocks experienced a complex structural sequence with mineralization occurring under greenschist facies conditions in the Late Archean (Baker et al., 2010). The deformation/mineralization sequence involves at least two major episodes of mineralization during D<sub>4</sub> (Table 1), which was characterized by dextral-normal extensional shear (Blenkinsop et al., 2009), accompanied by a late CO<sub>2</sub> fluid influx associated with Te, Ag, and As (Sung et al., 2007; Baker et al., 2010). A more recent example of strike-slip dominated lode gold mineralization is provided by the latest Eocene-Oligocene mineralization in the Daping gold deposit, containing one of the largest resources in the Ailaoshan gold belt, Eastern China, which is related to the right lateral Red River fault (Hou and Cook, 2009; Sun et al., 2009).

Clear examples of hydrothermal gold mineralization during extension, well below the top 2 km of the crust where epithermal deposits form, are reported from the Dolgelau Gold Belt in North Wales, where the Clogau-St Davids (100 000 oz Au produced) and Gwynfynydd (50 000 oz Au) mines are located (Platten and Dominy, 2009). The gold-bearing quartz veins in the gold belt consist of an ENE-WSW array of steeply dipping laminated quartz-carbonate veins hosted in Cambrian mudstones at low greenschist facies conditions (Dominy et al., 1996a, b). The veins are hosted within normal faults that pre-date the veining. Originally considered to have a late to post-tectonic

1 timing (Shepherd and Allen, 1985), detailed work by Platten and Dominy (1999) shows that the  
2 gold mineralization predates an Acadian slaty cleavage. A critical piece of evidence is the presence  
3 of barren lenticular quartz veins, which cross-cut the gold-bearing quartz veins, and are related to  
4 the sub-horizontal shortening and sub-vertical extension of the cleavage and fold forming event.  
5 The barren quartz veins also cut post-mineralization “Clogau Stone” dykes, confirming the early  
6 timing for the mineralization. Narrow zones of alteration around the veins include phyllosilicates,  
7 carbonate and silica (Dominy et al., 1996a, b). Low salinity aqueous-CH<sub>4</sub>- CO<sub>2</sub> fluids suggest ore  
8 formation at 300-320°C, 180 MPa (Bottrell et al., 1988). Gold precipitation was by destabilization  
9 of either chloride or sulfide complexes, as a result of fluid interaction with host-rock graphite  
10 (Shepherd et al., 1991). The veins formed due to fluid overpressure in an NNW-SSE extensional  
11 event, contemporary with Ordovician volcanism and development of the Lower Paleozoic Welsh  
12 basin (Kokelaar, 1988) that predates the Acadian orogeny.  
13  
14  
15  
16  
17  
18  
19  
20  
21  
22

23 Detailed structural analysis of several hundred mine working in the Barberton greenstone belt  
24 shows that almost all mineralization was associated with normal faulting, with a dominantly NW-  
25 SE extension direction. This mineralization event is dated at ~ 3015 Ma, 85 Ma after granite  
26 batholith emplacement and stabilization of the craton, at the time that the Witwatersrand basin  
27 opened (Dirks et al., 2013, 2009; Munyai et al., 2011). In large mines like Sheba and New Consort  
28 (together > 6Moz) in Barberton, the normal faults overprint/reactivate thrusts that were linked to  
29 accretionary events which occurred ~200 Ma before gold mineralization. In the Nyankanga gold  
30 deposit (~10 Moz), Geita greenstone belt, Tanzania, mineralization occurred during normal  
31 reactivation of the reverse Nyankanga fault-shear zone (Sanislav et al., 2015), and at the Geita Hill  
32 gold deposit (~3 Moz), there is evidence to link at least some of the mineralization to normal fault  
33 movement in the last deformation event recorded in the deposit which appears to have occurred  
34 ~40-50 Ma after the accretionary stages in the greenstone belt (Sanislav et al., 2017). This is well-  
35 illustrated by sub-vertical, approximately E-W trending, mineralized quartz veins that overprint  
36 earlier structures and are surrounded by a gold-rich alteration halo of quartz, biotite, k-feldspar and  
37 pyrite (van Ryt et al., 2017).  
38  
39  
40  
41  
42  
43  
44  
45  
46  
47  
48  
49  
50  
51  
52

53 Extensional structural controls on gold mineralization in the Yilgarn craton have been advocated by  
54 several studies (Davis and Maidens, 2003; Czarnota et al., 2007; Weinberg and van der Borgh,  
55 2008; Blewett et al., 2010), and are commonly linked to granite intrusion. Marvel Loch deposit (4  
56 Moz) within the Southern Cross Greenstone Belt, Western Australia, is an example of major gold-  
57 mineralization associated with post compressional, extension-related strike and normal slip  
58  
59  
60  
61  
62  
63  
64  
65

1 movement. Some gold mineralization is hosted in veins developed during NNW-SSE directed  
2 shortening coupled with preferential alteration of a primary gabbro by albite-arsenopyrite-  
3 associated gold mineralization that post-dates peak metamorphic, calc-silicate assemblages. The  
4 most significant gold mineralization is, however, in vein quartz developed at intersections with NW  
5 and N-S trending structures that concentrated veins during NE-SW extension (Nugus, 1999; Witt  
6 2000).  
7  
8  
9

10  
11  
12 Warren et al. (2015) found that at the Castle Hill gold camp, Coolgarde domain, W. Australia, both  
13 granite intrusion and later gold mineralization was localized by a bend in the Kunanalling Shear  
14 Zone, and that gold mineralization occurred in localized extensional structures during a period of  
15 NW-SE compression. They cautioned that local structures may not reflect the regional tectonic  
16 picture. This is unlikely to be the case for the Barberton, Geita or Sunrise Dam examples above,  
17 where normal components of deformation can be seen on scales of km and cannot therefore be  
18 considered as local deformation effects.  
19  
20  
21  
22  
23  
24  
25  
26  
27

28 Present day and recent tectonics in accretionary and collisional orogens may give some useful  
29 insights. Accretionary orogens can be divided into advancing and retreating types ( Royden, 1993;  
30 Cawood and Buchan, 2007). Where the velocity of slab retreat (rollback) is less than that of the  
31 overriding plate, advancing orogens are created, characterized by shortening and uplift: this  
32 situation arises due to coupling between the subducting and overriding plates, which can be due to  
33 flat slab subduction, terrane accretion, or global plate reorganization. Today's eastern Pacific  
34 margin orogens are of this type. Where slab retreat is more rapid than the velocity of the overriding  
35 plate, extension occurs in the overriding plate, as seen in most Western Pacific margins today.  
36 Tectonic switching between advancing and retreating modes can occur: for example, the Lachlan  
37 fold belt in SE Australia was in long-term retreat mode, punctuated by episodic advancing  
38 orogenesis (Collins, 2002). Most orogens probably involve oblique motions in addition to  
39 convergence or divergence (Cawood et al., 2009). Collisional orogenies may undergo extension  
40 following crustal thickening (e.g. Platt and Vissers, 1989) or as a possible consequence of slab  
41 break-off and asthenospheric upwelling (Davies and von Blanckenburg, 1995).  
42  
43  
44  
45  
46  
47  
48  
49  
50  
51  
52  
53  
54  
55  
56

57 Figure 12 shows in situ stress states in the Asia region, encompassing the collisional orogeny of the  
58 Himalayas, the intracontinental deformation of the Himalayan hinterland, and the accretionary  
59 orogens of the Sumatra-Indonesian and Philippine arcs (Heidbach et al., 2008). It is striking that all  
60  
61  
62  
63  
64  
65



of these tectonic settings show a variety of stress states, commonly in close proximity, especially along the arcs. In a total of 3688 stress determinations, normal and strike slip stresses together (53%) amount to more than reverse stress measurements, even in these archetypal convergent settings. The documentation of gold deposits with extensional or strike-slip tectonics on a greater than local scale suggests that gold deposits can form in several possible stress states and tectonic situations. Such a variety of stress states is also more compatible with known conditions in both accretionary and collisional orogens. An important insight from the case studies above is that structural controls on gold deposits may reflect regional tectonic settings, or they may have quite different local tectonics. It is inadvisable either to infer a regional picture from a deposit scale analysis, or, visa versa, to infer likely deposit scale tectonics from a regional context.

## **Workflow**

The suggested workflow (Fig. 13) includes the main methods used in structural analysis of gold deposits, arranged in order of a classic structural geology approach. However, we wish to emphasise that this is not a prescription. Some methods suggested may be simply inapplicable e.g. if core is not available. The following brief comments on the workflow are mainly intended to give examples and indicate some useful resources.

### ***Data Acquisition***

In the context of mapping for structural analysis of gold deposits, it is especially important to focus on lithology and alteration, because of their significance for rheology and fluid flow (e.g. Kisters et al., 2000) in addition to the usual mapping of contacts, fabrics and deformation zones. It is worth spending a significant amount of time to define a consistent lithostratigraphy, for which cores may be the best resource since they provide continuous material that is commonly fresh.

Even the most fragmentary and weathered outcrop can be invaluable in regions of poor outcrop. There is commonly a good case for mapping on several different scales because outcrops can vary from complete, e.g. in three-dimensions underground, to very poor at surface. Drone or Lidar data are invaluable in open pits where access is commonly problematic, and underground where such data is also being increasingly acquired for safety reasons. In most production-orientated situations it is important to map at frequent intervals as pits and stopes advance rapidly.

Core analysis is commonly vital for evaluating structures and their variation in 3D (Vearncombe and Vearncombe, 1998; Marjoribanks, 2010; Holcombe, 2016). Lineations of any type can be

1 essential clues to directions of increased permeability, but are commonly overlooked in core  
2 logging, perhaps because of lack of familiarity with measuring techniques. One of the benefits of  
3 working with cores is the complete 3D exposure offered by a core, in which case it is also quite  
4 straightforward to look for planes of maximum asymmetry, which will be perpendicular to vorticity  
5 vectors: these too can be measured as lines (Blenkinsop et al., 2015). It is greatly preferable to work  
6 with whole core because of the greater sampling volume, and therefore to log before core is  
7 sampled, even though methods exist for dealing with half core (Blenkinsop and Doyle, 2010).  
8  
9

10  
11  
12  
13  
14 Microstructural analysis is useful for establishing pressures and temperatures of deformation,  
15 overprinting relationships, deformation mechanisms (e.g. Davis et al., 2010), and kinematic analysis  
16 (e.g. Blenkinsop and Doyle, 2014; Blenkinsop et al., 2017). It is also invaluable for relating  
17 deformation events to mineralization and paragenesis (e.g. Cox et al., 1995; Morey et al., 2007), yet  
18 many structural studies of gold mineralization omit this important step (Davis, 2002), perhaps  
19 because making and analyzing thin sections adds extra time. However, this time is well spent.  
20  
21  
22  
23  
24  
25

26  
27  
28 Lithological, structural, geophysical and geochemical data need to be readily visible in relation to  
29 each other, and readily viewed at different scales and from different orientations. Such capabilities  
30 are inherent in mining software packages, and increasingly in virtual globes such as Google Earth  
31 and Worldwind, and now even in GIS packages. Interactive 3D presentations of data are highly  
32 effective at communicating complex spatial relationships on all scales: microtomographic images  
33 can be combined with outcrop scale photogrammetry (including invaluable drone-acquired imagery;  
34 Bemis et al., 2014) and regional 3D models.  
35  
36  
37  
38  
39  
40  
41  
42  
43  
44

### 45 ***Geometric, Kinematic, Dynamic and Rheological Analysis***

46 An accurate 3D geometrical model of structures and mineralization is an essential starting point for  
47 kinematic analysis. Geometrical modeling requires input from maps and drilling, and can be done  
48 manually or through implicit methods (Cowan et al., 2003; Hill et al., 2014). Structural domains,  
49 first introduced at least 60 years ago (Weiss and McIntyre, 1957), are still very useful for  
50 understanding spatial and temporal geometrical relationships (Miller and Wilson, 2004b), especially  
51 in large, complex ore deposits that are likely to be geometrically, kinematically and dynamically  
52 heterogenous (e.g. Baker et al., 2010). Network geometry can be analyzed from digital data in a  
53 semi-automatic way (Healy et al., 2016).  
54  
55  
56  
57  
58  
59  
60  
61  
62  
63  
64  
65

1 In building a complex deformation chronology based on cross-cutting or overprinting relationships,  
2 younging tables are an invaluable way to organize and present data (Angelier, 1991; Potts and  
3 Reddy, 2000). Kinematic analysis of deformation zones in multiple orientations is well established  
4 for fault zones (Marrett and Allmendinger, 1990), but the same techniques can also be applied to  
5 mineralized shear zones (Blenkinsop and Doyle, 2014).  
6  
7  
8  
9

10  
11  
12 There are many methods available for dynamic or paleostress analysis, which mainly differ in the  
13 extent to which different stress tensors can be separated from the data. For single stress states, the  
14 following are among some of the most recent: Lisle, (1988); Delvaux, (2012); Thakur et al., (2017).  
15 For separating multiple stress states, see the following: Yamaji et al., (2010); Hansen et al., (2015);  
16 Lisle and Vandycke, (1996); Lisle and Orife, (2002); Liesa and Lisle, (2004); Shan and Fry, (2005);  
17 Žalohar and Vrabec, (2007). There are some interesting methods that combine kinematic and  
18 dynamic approaches (e.g. Žalohar and Vrabec, 2008, 2010; Hansen, 2013). None of these methods  
19 deal with absolute stress or directly with pore fluid pressures. Fluid inclusion studies are very  
20 important for the latter (e.g. Boullier and Robert, 1992b; Robert et al., 1995).  
21  
22  
23  
24  
25  
26  
27  
28  
29  
30

31  
32 Rheological analysis of gold mineralization ideally relates stress to strain or strain rate over a range  
33 of time scales from the seconds of earthquake rupture to the thousands to tens of thousands of years  
34 required to form an ore deposit as discussed above. The best numerical modeling will be able to  
35 explore these aspects of deformation constrained by realistic rock properties and kinematic or  
36 dynamic boundary conditions determined from structural analysis (Schaubs and Zhao, 2002;  
37 Schaubs et al., 2006; McLellan et al., 2007; Potma et al., 2008). However, a major challenge to  
38 mechanical modeling in the context of mineral resources is to be able to combine discontinuous and  
39 continuous styles of deformation at a variety of scales. In particular, microcracking and brecciation  
40 are very difficult to model satisfactorily. The influence of chemical changes on mechanical  
41 properties is another level of complexity that is rarely achieved.  
42  
43  
44  
45  
46  
47  
48  
49  
50  
51

## 52 *Synthesis*

53  
54 An ideal synthesis to conclude the workflow would consist of a geological history in which each  
55 deformation event is understood from geometrical, kinematic, dynamic, and rheological view  
56 points, and gold mineralization can be tied to one or more specific points in this history. This  
57  
58  
59  
60  
61  
62  
63  
64  
65

1 requires integrating the classic structural geology approach with geochemistry, geophysics and  
2 above all geochronology. Such a synthesis, combined with a good understanding of regional  
3 geology, has very powerful predictive capacity. It is not surprising that large ore deposits can be  
4 the subject of several or even many PhD studies, given this preferred end point, and nor is it  
5 surprising that there is a continual search for magic bullets that can short-cut the workflow.  
6  
7  
8  
9

## 10 11 **Conclusions**

12 Hydrothermal gold deposits have several characteristic features, including strong structural control  
13 via deformation-induced permeability related to deformation zone networks, fluid-rock interaction  
14 resulting in a zoned pattern of alteration, and evidence for a protracted sequence of deformation  
15 with cyclic changes in stress and fluid flow. The syn-mineralization kinematics of deposits as a  
16 group is truly variable, from pure reverse to pure normal senses of movement on deformation zones.  
17  
18 Structural controls on these deposits are one of their most distinctive features.  
19  
20  
21  
22  
23  
24  
25  
26  
27

28 Geometrical analysis of structures, networks and ore bodies is the most basic step in analyzing  
29 hydrothermal gold deposits. Geometrical analysis can now include new techniques of analyzing  
30 network topology, as well as a more quantitative approach to relating ore body geometry to  
31 deformation. Kinematic analysis is also essential for the latter purpose, as well as to relate deposit-  
32 scale features to regional tectonics. Several examples show that it is important to move beyond the  
33 Ramsay and Graham simple shear paradigm for shear zone kinematics; inclusion of significant pure  
34 shear components in deformation zones can change relationships between ore bodies, lineations,  
35 and vorticity vectors, and this is crucial for predicting ore body geometry and in numerical  
36 mechanical modeling. An appreciation that many deformation zone networks are polygonal, which  
37 is to be expected in a general state of strain, may also be important because of their influence on  
38 fluid pathways.  
39  
40  
41  
42  
43  
44  
45  
46  
47  
48  
49  
50

51 A dynamic analysis of hydrothermal gold deposits will assess pore fluid pressure and stress,  
52 preferably using numerical mechanical models. The involvement of fluids in slow slip, and the scale  
53 of slip increments in vein textures, suggests that slow slip is likely to be involved in mineralization.  
54 Numerical mechanical models have considerable predictive power, but they do not yet successfully  
55 encompass the likely range of slip speeds on faults, nor deal effectively with cyclic behavior or the  
56 complexity of overprinting that obscures early dynamic behavior.  
57  
58  
59  
60  
61  
62  
63  
64  
65

1 Analysis of rheology is the key in many cases to understanding the structural controls on ore bodies,  
2 which are commonly located on rheological boundaries. Reactivation and multiple cycles of  
3 mineralization, sometimes separated by tens to hundreds of millions of years, is a feature of many  
4 deposits, including some of the largest. If inherited structures are weaker than intact rock, they can  
5 be reactivated in a variety of orientations. Slip and dilation tendency are useful techniques for  
6 analyzing propensity for reactivation.  
7  
8  
9

10  
11  
12  
13  
14 Stress states in all types of orogenic zones observed today are variable throughout the crust. A  
15 logical implication is that hydrothermal gold deposits formed and exhumed from previous orogenies  
16 will record a complex structural history. Unraveling that history, by breaking it down into each  
17 separate phase, is a traditional structural geology approach that is still essential in order to work out  
18 which phase or phases of deformation are associated with mineralization. Short time-scale stress  
19 changes associated with seismic or sub-seismic cycles within the same phase of deformation need to  
20 be distinguished from longer time scale switches in tectonic mode. Short time scale, cyclic changes  
21 are likely to be represented by numerous repetitions and mutually cross-cutting relationships  
22 between fault zones, veins and shear zones; longer time-scale tectonic switches will show a  
23 consistent structural paragenesis. There may be great variation in the scale over which a tectonic  
24 setting applies, and there may be rapid temporal changes, so that it is inadvisable to infer local  
25 tectonics from regional patterns, and visa versa.  
26  
27  
28  
29  
30  
31  
32  
33  
34  
35  
36  
37  
38  
39

40 New developments in structural geology that appear to have great promise for understanding gold  
41 deposit genesis and for exploration include the application of network and percolation theories, and  
42 non-equilibrium thermodynamics. The latter is a quantifiable systems approach, which integrates  
43 deformation (in the sense of displacements and strain), stress, fluids, heat and chemical reactions.  
44 The non-linear behavior of an ore-forming system leads to multifractal properties that can be  
45 measured and should have direct exploration implications. Even these characteristics, however, will  
46 need to be placed in a complete structural history.  
47  
48  
49  
50  
51  
52  
53  
54  
55  
56

## 57 **Acknowledgements**

58  
59 Discussions with Tim Baker, James Cleverley, Simon Dominy, Mark Doyle, John McLellan,  
60 Howard Poulsen and Dave Sanderson were helpful in developing some of the ideas in this article.  
61  
62  
63  
64  
65

1  
2  
3  
4  
5  
6  
7  
8  
9  
10  
11  
12  
13  
14  
15  
16  
17  
18  
19  
20  
21  
22  
23  
24  
25  
26  
27  
28  
29  
30  
31  
32  
33  
34  
35  
36  
37  
38  
39  
40  
41  
42  
43  
44  
45  
46  
47  
48  
49  
50  
51  
52  
53  
54  
55  
56  
57  
58  
59  
60  
61  
62  
63  
64  
65

Other formative influences were Bruce Hobbs, Alex Kisters, Alison Ord, Rick Sibson, Basil Tikoff, Julian Vearncombe and Steve Wojtal, though they do not necessarily endorse the contents. We are grateful to Geof Steed, and reviewers Howard Poulsen, Tim Baker and Steve Micklethwaite for helpful comments, and editor Julie Rowland for advice.

## References

- Allibone, A., Teasdale, J., Cameron, G., Etheridge, M., Uttley, P., Soboh, A., Appiah-Kubi, J., Adanu, A., Arthur, R., Mamphey, J., Odoom, B., Zuta, J., Tsikata, A., Pataye, F., Famiyeh, S., 2002a. Timing and structural controls on gold mineralization at the Bogoso mine, Ghana, West Africa. *Econ. Geol.* 97-5, 949-, 949–969.
- Allibone, A.H., McCuaig, T.C., Harris, D., Etheridge, M., Munroe, S., Byrne, D., 2002b. Chapter 4 Structural Controls on Gold Mineralization at the Ashanti Gold Deposit, Obuasi, Ghana. *Soc. Econ. Geol. Spec. Publ.* 9, 65–93.
- Anderson, E.M., 1905. The dynamics of faulting. *Trans. Edinburgh Geol. Soc.* 8, 387–402.  
doi:10.1144/transed.8.3.387
- Angelier, J., 1975. Sur l'analyse de mesures recueillies sans des sites faillés: l'utilité d'une confrontation entre les méthodes dynamiques et cinématiques. *Comptes Rendus l'Académie des Sci. Paris D218*, 1805–1808.
- Angelier, J., 1991. Analyse chronologique matricielle et succession régionale des événements tectoniques. *Comptes rendus l'Académie des Sci. Série 2, Mécanique, Phys. Chim. Sci. l'univers, Sci. la Terre* 312, 1633–1638.
- Arne, D.C., Bierlin, F.P., Morgan, J.W., Stein, H.J., 2001. Re-Os dating of sulfides associated with gold mineralization in Central Victoria, Australia. *Econ. Geol.*  
doi:10.2113/gsecongeo.96.6.1455
- Baker, T., Bertelli, M., Blenkinsop, T., Cleverly, J., McLellan, J.G., Nugus, M., Gillen, D., 2010. PTX conditions of fluids in the Sunrise Dam gold deposit, Western Australia, and implications for the interplay between deformation and fluids. *Econ. Geol.* 105, 873–894.
- Barnhoorn, A., Cox, S.F., Robinson, D.J., Senden, T., 2010. Stress- and fluid-driven failure during fracture array growth: Implications for coupled deformation and fluid flow in the crust. *Geology* 38, 779–782. doi:10.1130/G31010.1
- Bateman, R., Hagemann, S., 2004. Gold mineralisation throughout about 45 Ma of Archaean

orogenesis: Protracted flux of gold in the Golden Mile, Yilgarn craton, Western Australia. *Miner. Depos.* 39, 536–559. doi:10.1007/s00126-004-0431-2

1  
2  
3 Bemis, S.P., Micklethwaite, S., Turner, D., James, M.R., Akciz, S., T. Thiele, S., Bangash, H.A.,  
4 2014. Ground-based and UAV-Based photogrammetry: A multi-scale, high-resolution  
5 mapping tool for structural geology and paleoseismology. *J. Struct. Geol.* 69, 163–178.  
6 doi:10.1016/j.jsg.2014.10.007  
7  
8  
9

10 Ben-zion, Y., 2008. Collective Behavior of Earthquakes and Faults. *Rev. Geophys.* 46, 1–70.  
11 doi:10.1029/2008RG000260  
12  
13

14 Beroza, G.C., Ide, S., 2011. Slow Earthquakes and Nonvolcanic Tremor. *Annu. Rev. Earth Planet.*  
15 *Sci.* 39, 271–296. doi:10.1146/annurev-earth-040809-152531  
16  
17  
18

19 Bierlein, F.P., Maher, S., 2001. Orogenic disseminated gold in phanerozoic fold belts - Examples  
20 from Victoria, Australia and elsewhere. *Ore Geol. Rev.* 18, 113–148. doi:10.1016/S0169-  
21 1368(01)00019-1  
22  
23  
24

25 Bierlein, F.P., Groves, D.I., Goldfarb, R.J., Dubé, B., 2006. Lithospheric controls on the formation  
26 of provinces hosting giant orogenic gold deposits. *Miner. Depos.* 40, 874–886.  
27 doi:10.1007/s00126-005-0046-2  
28  
29  
30

31 Blenkinsop, T.G., 2004a. Orebody geometry in lode gold deposits from Zimbabwe: implications for  
32 fluid flow, deformation and mineralization. *J. Struct. Geol.* 26, 1293–1301.  
33 doi:10.1016/j.jsg.2003.11.010  
34  
35  
36

37 Blenkinsop, T.G., 2004b. Pure and Simple: A Practical Guide to Predicting Ore Body Geometry in  
38 Shear Zones, in: Dominy, S.C. (Ed.), *Mining and Resource Geology Symposium*. EGRU,  
39 James Cook University, Townsville, pp. 9–18.  
40  
41  
42

43 Blenkinsop, T., 2014. Scaling Laws for the Distribution of Gold, Geothermal, and Gas Resources.  
44 *Pure Appl. Geophys.* 2045–2056. doi:10.1007/s00024-014-0909-5  
45  
46

47 Blenkinsop, T.G., Frei, R., 1996. Archean and proterozoic mineralization and tectonics at the Renco  
48 mine (Northern Marginal Zone, Limpopo Belt, Zimbabwe). *Econ. Geol.* 91, 1225–1238.  
49 doi:10.2113/gsecongeo.91.7.1225  
50  
51  
52

53 Blenkinsop, T.G., Kadzviti, S., 2006. Fluid flow in shear zones: insights from the geometry and  
54 evolution of ore bodies at Renco gold mine, Zimbabwe. *Geofluids* 6, 334–345.  
55  
56

57 Blenkinsop, T.G., Doyle, M.G., 2010. A method for measuring the orientations of planar structures  
58 in cut core. *J. Struct. Geol.* 32, 741–745. doi:10.1016/j.jsg.2010.04.011  
59  
60

61 Blenkinsop, T.G., Doyle, M.G., 2014. Structural controls on gold mineralization on the margin of  
62  
63  
64  
65

the Yilgarn craton, Albany–Fraser orogen: The Tropicana deposit, Western Australia. *J. Struct. Geol.* 67, 189–204. doi:10.1016/j.jsg.2014.01.013

1  
2  
3 Blenkinsop, T.G., Schmidt Mumm, A., Kumi, R., Sangmor, S., 1994. Structural geology of the  
4 Ashanti gold mine. *Geol. Jahrb. D* 100, 131–153.

5  
6  
7 Blenkinsop, T.G., Oberthür, T., Mapeto, O., 2000. Gold mineralization in the Mazowe area, Harare-  
8 Bindura-Shamva greenstone belt, Zimbabwe: I. Tectonic controls on mineralization. *Miner.*  
9 *Depos.* 35, 126–137. doi:10.1007/s001260050011

10  
11  
12 Blenkinsop, T., Kröner, A., Chiwara, V., 2004. Single stage, late Archaean exhumation of  
13 granulites in the Northern Marginal Zone, Limpopo Belt, Zimbabwe, and relevance to gold  
14 mineralization at Renco mine. *South African J. Geol.* 107, 377–396.

15  
16  
17 Blenkinsop, T., Kreuzer, O.P., McLellan, J., Baker, T., 2009. Sunrise Dam Gold Mine , Western  
18 Australia : Mechanical Controls on an Archean Lode Gold Hydrothermal System, in:  
19 Williams, P.J. (Ed.), *Proceedings of the Tenth Biennial SGA Meeting*. Australian Institute of  
20 Mining and Metallurgy, Townsville, pp. 800–802.

21  
22  
23 Blenkinsop, T.G., Doyle, M., Nugus, M., 2015. A unified approach to measuring structures in  
24 orientated drill core, in: Richards, F. L., Richardson, N. J., Rippington, S.  
25 J., Wilson, R.W. & Bond, C. E. (Eds) *Industrial Structural Geology: Principles, Techniques and*  
26 *Integration*. Geological Society, London, Special Publications, 421,  
27 <http://dx.doi.org/10.1144/SP421.1>. doi:10.1144/SP421.1

28  
29  
30 Blenkinsop, T., Tripp, G., Gillen, D., 2018. The relation between mineralization and tectonics at the  
31 Kainantu gold-copper deposit, Papua New Guinea. *Spec. Publ. Geol. Soc.* 453.

32  
33  
34 Blewett, R.S., Czarnota, K., Henson, P.A., 2010. Structural-event framework for the eastern Yilgarn  
35 Craton, Western Australia, and its implications for orogenic gold. *Precambrian Res.* 183, 203–  
36 229. doi:<http://dx.doi.org/10.1016/j.precamres.2010.04.004>

37  
38  
39 Bons, P.D., 2001. The formation of large quartz veins by rapid ascent of fluids in mobile  
40 hydrofractures. *Tectonophysics* 336, 1–17. doi:[http://dx.doi.org/10.1016/S0040-](http://dx.doi.org/10.1016/S0040-1951(01)00090-7)  
41 [1951\(01\)00090-7](http://dx.doi.org/10.1016/S0040-1951(01)00090-7)

42  
43  
44 Bottrell, S.H., Shepherd, T.J., Yardley, B.W.D., Dubessy, J., 1988. Fluid Inclusion Model for the  
45 Genesis of the Ores of the Dalgellau Gold Belt, North Wales. *J. Geol. Soc. London* 145, 139–  
46 145.

47  
48  
49 Boullier, A.-M., Robert, F., 1992. Palaeoseismic events recorded in Archaean gold-quartz vein  
50 networks, Val d’Or, Abitibi, Quebec, Canada. *J. Struct. Geol.* 14, 161–179.



- 1 Brace, W.F., 1980. Permeability of crystalline and argillaceous rocks. *Int. J. Rock Mech. Min. Sci.*  
2  
3 *Geomech. Abstr.* 17, 241–251. doi:[10.1016/0148-9062\(80\)90807-4](https://doi.org/10.1016/0148-9062(80)90807-4)  
4
- 5 Calais, E., d'Oreye, N., Albaric, J., Deschamps, A., Delvaux, D., Déverchère, J., Ebinger, C.,  
6  
7 Ferdinand, R.W., Kervyn, F., Macheyeke, A.S., Oyen, A., Perrot, J., Saria, E., Smets, B.,  
8  
9 Stamps, D.S., Wauthier, C., 2008. Strain accommodation by slow slip and dyking in a youthful  
10  
11 continental rift, East Africa. *Nature* 456, 783–787. doi:[10.1038/nature07478](https://doi.org/10.1038/nature07478)  
12
- 13 Carvell, J., Blenkinsop, T., Clarke, G., Tonelli, M., 2014. Scaling, kinematics and evolution of a  
14  
15 polymodal fault system: Hail Creek Mine, NE Australia. *Tectonophysics* 632, 138–150.  
16  
17 doi:[10.1016/j.tecto.2014.06.003](https://doi.org/10.1016/j.tecto.2014.06.003)  
18
- 19 Cawood, P.A., Buchan, C., 2007. Linking accretionary orogenesis with supercontinent assembly.  
20  
21 *Earth- Sci. Rev.* 82, 217–256.  
22
- 23 Cawood, P.A., Kroner, A., Collins, W.J., Kusky, T.M., Mooney, W.D., Windley, B.F., 2009.  
24  
25 Accretionary orogens through Earth history. *Geol. Soc. London, Spec. Publ.* 318, 1–36.  
26  
27 doi:[10.1144/SP318.1](https://doi.org/10.1144/SP318.1)  
28
- 29 Chamberlain, C.J., Shelly, D.R., Townend, J., Stern, T., 2014. Low-frequency earthquakes reveal  
30  
31 punctuated slow slip on the deep extent of the Alpine Fault, New Zealand. *Geochemistry,*  
32  
33 *Geophys. Geosystems* n/a-n/a. doi:[10.1002/2014GC005436](https://doi.org/10.1002/2014GC005436)  
34
- 35 Chang, C., Haimson, B., 2012. A Failure Criterion for Rocks Based on True Triaxial Testing. *Rock*  
36  
37 *Mech. Rock Eng.* 45, 1007–1010. doi:[10.1007/s00603-012-0280-8](https://doi.org/10.1007/s00603-012-0280-8)  
38
- 39 Choukroune, P., Gapais, D., 1983. Strain Patterns in Rocks Strain pattern in the Aar Granite  
40  
41 (Central Alps): Orthogneiss developed by bulk inhomogeneous flattening. *J. Struct. Geol.* 5,  
42  
43 411–418. doi:[http://dx.doi.org/10.1016/0191-8141\(83\)90027-5](http://dx.doi.org/10.1016/0191-8141(83)90027-5)  
44
- 45 Collins, W.J., 2002. Hot orogens, tectonic switching, and creation of the continental crust. *Geology*  
46  
47 30, 535–538.  
48
- 49 Colvine, A.C., 1989. An empirical model for the formation of Archean gold deposits: products of  
50  
51 final cratonization of the Superior Province, Canada. *Econ. Geol. Monogr.* 6, 37–53.  
52  
53
- 54 Cowan, E.J., Beatson, R.K., Ross, H.J., Fright, W.R., McLennan, T.J., Evans, T.R., Carr, J.C.,  
55  
56 Lane, R.G., Bright, D. V, Gillman, A.J., 2003. Practical implicit geological modelling, in: *Fifth*  
57  
58 *International Mining Geology Conference*. Australian Institute of Mining and Metallurgy  
59  
60 Bendigo, Victoria, pp. 17–19.  
61
- 62 Cox, S.F., 1999. Deformational controls on the dynamics of fluid flow in mesothermal gold  
63  
64  
65

systems. *Geol. Soc. London, Spec. Publ.* 155, 123–140. doi:10.1144/GSL.SP.1999.155.01.10

1 Cox, S.F., Ruming, K., 2004. The St Ives mesothermal gold system, Western Australia—a case of  
2 golden aftershocks? *J. Struct. Geol.* 26, 1109–1125.

3  
4 doi:http://dx.doi.org/10.1016/j.jsg.2003.11.025  
5

6  
7 Cox, S.F., Sun, S.S., Etheridge, M.A., Wall, V.J., Potter, T.F., 1995. Structural and geochemical  
8 controls on the development of turbidite-hosted gold quartz vein deposits, Wattle Gully mine,  
9 central Victoria, Australia. *Econ. Geol.* 90, 1722–1746.  
10

11  
12  
13 Craw, D., Windle, S.J., Angus, P. V., 1999. Gold mineralization without quartz veins in a ductile-  
14 brittle shear zone, Macraes Mine, Otago Schist, New Zealand. *Miner. Depos.* 34, 382–394.

15  
16 doi:10.1007/s001260050211  
17

18  
19 Czarnota, K., Blewett, R.S., Champion, D.C., Henson, P.A., Cassidy, K.F., 2007. Significance of  
20 extensional tectonics in orogenic gold systems: an example from the Eastern Goldfields  
21 Superterrane, Yilgarn Craton, Australia, *Digging Deeper*, Vols 1 and 2: *Digging Deeper*.  
22

23  
24  
25 Czarnota, K., Blewett, R.S., Goscombe, B., 2010. Predictive mineral discovery in the eastern  
26 Yilgarn Craton, Western Australia: An example of district scale targeting of an orogenic gold  
27 mineral system. *Precambrian Res.* 183, 356–377. doi:10.1016/j.precamres.2010.08.014  
28

29  
30  
31 Davies, H., von Blanckenburg, F., 1995. Slab breakoff: A model of lithosphere detachment and its  
32 test in the magmatism and deformation of collisional orogens. *Earth Planet. Sci. Lett.* 129, 85–  
33 102. doi:10.1016/0012-821X(94)00237-S  
34

35  
36  
37 Davis, B.K., 2002. *Applied Structural Geology for Exploration and Mining*. Aust. Inst. Geosci.  
38 Bull. 36, 242.  
39

40  
41 Davis, B.K., Maidens, E., 2003. Archaean orogen-parallel extension: Evidence from the northern  
42 Eastern Goldfields Province, Yilgarn Craton, in: *Precambrian Research*. pp. 229–248.  
43

44  
45 Davis, B.K., Blewett, R.S., Squire, R., Champion, D.C., Henson, P. a., 2010a. Granite-cored domes  
46 and gold mineralisation: Architectural and geodynamic controls around the Archaean Scotia-  
47 Kanowna Dome, Kalgoorlie Terrane, Western Australia. *Precambrian Res.* 183, 316–337.  
48  
49 doi:10.1016/j.precamres.2010.01.011  
50

51  
52  
53 Davis, B.K., Blewett, R.S., Squire, R., Champion, D.C., Henson, P. a., 2010b. Granite-cored domes  
54 and gold mineralisation: Architectural and geodynamic controls around the Archaean Scotia-  
55 Kanowna Dome, Kalgoorlie Terrane, Western Australia. *Precambrian Res.* 183, 316–337.  
56  
57 doi:10.1016/j.precamres.2010.01.011  
58

- 1 Delvaux, D., 2012. Release of program Win-Tensor 4.0 for tectonic stress inversion: statistical  
2 expression of stress parameters, in: Geophysical Research Abstracts.  
3  
4 Dipple, G.M., Ferry, J.M., 1992. Metasomatism and fluid flow in ductile fault zones. *Contrib. to*  
5 *Mineral. Petrol.* 112, 149–164. doi:10.1007/BF00310451  
6  
7 Dirks, P.H.G.M., Charlesworth, E.G., Munyai, M.R., 2009. Cratonic extension and Archaean gold  
8 mineralisation in the Sheba-Fairview mine, Barberton Greenstone Belt, South Africa.  
9 *South African J. Geol.* 112, 291–316.  
10  
11 Dirks, P.H.G.M., Charlesworth, E.G., Munyai, M.R., Wormald, R., 2013. Stress analysis, post-  
12 orogenic extension and 3.01Ga gold mineralisation in the Barberton Greenstone Belt, South  
13 Africa. *Precambrian Res.* 226, 157–184. doi:10.1016/j.precamres.2012.12.007  
14  
15 Dominy, S.C., Phelps, R.F.G., Camm, G.S., 1996a. Geological controls on gold grade distribution  
16 in Chidlaw link zone, Gwynfynydd mine, Dolgellau, north Wales. *Trans. Inst. Min. Metall.*  
17 *Sect. B. Appl. Earth Sci.* 105, B151.  
18  
19 Dominy, S.C., Phelps, R.F.G., Guard, C.L., 1996b. Geology and exploitation of complex gold-  
20 bearing veins in the Gwynfynydd mine, Dolgellau, North Wales, U.K. *Br. Min.* 57, 70–91.  
21  
22 Dube, B., Poulsen, H., Guha, J., 1989. The effects of layer anisotropy on auriferous shear zones; the  
23 Norbeau Mine, Quebec. *Econ. Geol.* 84, 871–878. doi:10.2113/gsecongeo.84.4.871  
24  
25 Eisenlohr, B.N., Groves, D., Partington, G.A., 1989. Crustal-scale shear zones and their significance  
26 to Archaean gold mineralization in Western Australia. *Miner. Depos.* 24, 1–8.  
27 doi:10.1007/BF00206714  
28  
29 Fagereng, A., Sibson, R.H., 2010. Melange rheology and seismic style. *Geology* 38, 751–754.  
30 doi:10.1130/G30868.1  
31  
32 Fagereng, Å., Remitti, F., Sibson, R.H., 2011. Incrementally developed slickenfibers — Geological  
33 record of repeating low stress-drop seismic events? *Tectonophysics* 510, 381–386.  
34 doi:http://dx.doi.org/10.1016/j.tecto.2011.08.015  
35  
36 Farrell, N.J.C., Healy, D., Taylor, C.W., 2014. Anisotropy of permeability in faulted porous  
37 sandstones. *J. Struct. Geol.* 63, 50–67. doi:10.1016/j.jsg.2014.02.008  
38  
39 Ford, A., Blenkinsop, T., McLellan, J., 2009. Factors affecting fluid flow in strike-slip fault  
40 systems: coupled deformation and fluid flow modelling with application to the western Mount  
41 Isa Inlier, Australia. *Geofluids* 1–22. doi:10.1111/j.1468-8123.2008.00219.x  
42  
43 Fossen, H., 1993. The deformation matrix for simultaneous simple shearing, pure shearing and  
44 volume change, and its application to transpression-transension tectonics. *J. Struct. Geol.* 15,

413–422.

- 1 Fyfe, W.S., Kerrich, R., 1976. Geochemical prospecting: Extensive versus intensive factors. *J.*  
2 *Geochemical Explor.* 6, 177–192.  
3  
4
- 5 Gapais, D., Bale, P., Choukroune, P., Cobbold, P., Mahjoub, Y., Marquer, D., 1987. Shear Criteria  
6 in Rocks Bulk kinematics from shear zone patterns: some field examples. *J. Struct. Geol.* 9,  
7 635–646. doi:[http://dx.doi.org/10.1016/0191-8141\(87\)90148-9](http://dx.doi.org/10.1016/0191-8141(87)90148-9)  
8  
9
- 10 Goldfarb, R.J., Groves, D.I., Gardoll, S., 2001. Orogenic gold and geologic time: a global synthesis.  
11 *Ore Geol. Rev.* 18, 1–75. doi:[http://dx.doi.org/10.1016/S0169-1368\(01\)00016-6](http://dx.doi.org/10.1016/S0169-1368(01)00016-6)  
12  
13  
14
- 15 Goldfarb, R.J., Baker, T., Dube, B., Groves, D.I., Hart, C.J., Gosselin, P., 2005. Distribution,  
16 character, and genesis of gold deposits in metamorphic terranes. *Econ. Geol.* 100th Anni.  
17  
18
- 19 Gomberg, J., 2010. Slow-slip phenomena in Cascadia from 2007 and beyond: A review. *Geol. Soc.*  
20 *Am. Bull.* 122, 963–978. doi:10.1130/B30287.1  
21  
22
- 23 Groves, D., Phillips, G., 1987. The genesis and tectonic control on Archaean gold deposits of the  
24 western Australian shield—a metamorphic replacement model. *Ore Geol. Rev.* 2, 287–322.  
25 doi:10.1016/0169-1368(87)90009-6  
26  
27  
28
- 29 Groves, D.I., Goldfarb, R.J., Gebre-Mariam, M., Hagemann, S.G., Robert, F., 1998. Orogenic gold  
30 deposits: A proposed classification in the context of their crustal distribution and relationship  
31 to other gold deposit types. *Ore Geol. Rev.* 13, 7–27. doi:[http://dx.doi.org/10.1016/S0169-](http://dx.doi.org/10.1016/S0169-1368(97)00012-7)  
32 [1368\(97\)00012-7](http://dx.doi.org/10.1016/S0169-1368(97)00012-7)  
33  
34  
35  
36
- 37 Groves, D., Goldfarb, R., Robert, F., Hart, C., 2003. Gold Deposits in Metamorphic Belts :  
38 Overview of Current Understanding , Outstanding Problems , Future Research , and  
39 Exploration Significance. *Econ. Geol.* 98, 1–29.  
40  
41  
42
- 43 Gustafson, L.B., 1989. SEG distinguished lecture in applied geology the importance of structural  
44 analysis in gold exploration. *Econ. Geol.* 84, 987–993. doi:10.2113/gsecongeo.84.4.987  
45  
46  
47
- 48 Hansen, J.-A., 2013. Direct inversion of stress, strain or strain rate including vorticity: A linear  
49 method of homogenous fault–slip data inversion independent of adopted hypothesis. *J. Struct.*  
50 *Geol.* 51, 3–13. doi:10.1016/j.jsg.2013.03.014  
51  
52  
53
- 54 Hansen, J.-A., Bergh, S.G., Osmundsen, P.T., Redfield, T.F., 2015. Stress inversion of  
55 heterogeneous fault-slip data with unknown slip sense: An objective function algorithm  
56 contouring method. *J. Struct. Geol.* 70, 119–140. doi:10.1016/j.jsg.2014.11.005  
57  
58  
59
- 60 Healy, D., Blenkinsop, T.G., Timms, N.E., Meredith, P.G., Mitchell, T.M., Cooke, M.L., 2015.  
61 Polymodal faulting: Time for a new angle on shear failure. *J. Struct. Geol.* 80, 57–71.  
62  
63  
64  
65

doi:10.1016/j.jsg.2015.08.013

- 1 Healy, D., Rizzo, R.E., Cornwell, D.G., Farrell, N.J.C., Watkins, H., Timms, N.E., Gomez-Rivas,  
2 E., Smith, M., 2016. FracPaQ: A MATLAB™ toolbox for the quantification of fracture  
3 patterns. *J. Struct. Geol.* 95, 1–16. doi:10.1016/j.jsg.2016.12.003  
4  
5  
6  
7 Heard, H.C., 1960. Transition from Brittle Fracture to Ductile Flow in Solenhofen Limestone as a  
8 Function of Temperature, Confining Pressure, and Interstitial Fluid Pressure, in: *Geological*  
9 *Society of America Memoir 79*. Geological Society of America, pp. 193–226.  
10  
11  
12  
13 doi:10.1130/MEM79-p193  
14  
15 Heidbach, O., Tingay, M., Barth, A., Reinecker, J., Kurfeß, D., Müller, B., 2008. The World Stress  
16 Map database release 2008. doi:10.1594/GFZ.WSM.Rel2008  
17  
18  
19 Hill, E.J., Oliver, N.H.S., Cleverley, J.S., Nugus, M.J., Carswell, J., Clark, F., 2014.  
20  
21  
22  
23  
24  
25  
26  
27  
28  
29  
30  
31  
32  
33  
34  
35  
36  
37  
38  
39  
40  
41  
42  
43  
44  
45  
46  
47  
48  
49  
50  
51  
52  
53  
54  
55  
56  
57  
58  
59  
60  
61  
62  
63  
64  
65
- Hobbs, B., Ord, A., Gorczyk, W., Gessner, K., 2012. Nonlinear and non-equilibrium  
thermodynamics without the complex mathematics by 1–53.
- Hodgson, C.J., 1989. Patterns of Mineralization, in: Bursnall, J.T. (Ed.), *Mineralization and Shear  
Zones: Short Course Notes Volume 6*. Geological Association of Canada, Montreal, pp. 51–88.
- Holcombe, R.J., 2016. Mapping and structural geology in mineral exploration: where theory hits the  
fan. *HCOV Global*.
- Holyland, P.W., Ojala, V.J., 1997. Computer-aided structural targeting in mineral exploration: Two-  
and three-dimensional stress mapping. *Aust. J. Earth Sci.* 44, 421–432.  
doi:10.1080/08120099708728323
- Hou, Z., Cook, N.J., 2009. Metallogensis of the Tibetan collisional orogen: A review and  
introduction to the special issue. *Ore Geol. Rev.* 36, 2–24.  
doi:10.1016/j.oregeorev.2009.05.001
- Hudleston, P., 1999. Strain compatibility and shear zones: is there a problem? *J. Struct. Geol.* 21,  
923–932. doi:http://dx.doi.org/10.1016/S0191-8141(99)00060-7
- Ingebritsen, S.E., Manning, C.E., 2010. Permeability of the continental crust : dynamic variations  
inferred from seismicity and metamorphism. *Geofluids* 10, 193–205. doi:10.1111/j.1468-  
8123.2010.00278.x
- Jelsma, H.A., Huizenga, J.M., Touret, J.L.R., 1998. Fluids and epigenetic gold mineralization at

Shamva Mine, Zimbabwe: a combined structural and fluid inclusion study. *J. African Earth Sci.* 27, 55–70.

Jia, Y., Kerrich, R., 2000. Giant quartz vein systems in accretionary orogenic belts : the evidence for a metamorphic fluid origin from N 15 N and N 13 C studies. *Earth Planet. Sci. Lett.* 184, 211–224.

Jiang, D., Williams, P.F., 1998. High-strain zones: a unified model. *J. Struct. Geol.* 20, 1105–1120. doi:[http://dx.doi.org/10.1016/S0191-8141\(98\)00025-X](http://dx.doi.org/10.1016/S0191-8141(98)00025-X)

Jolivet, R., Candela, T., Lasserre, C., Renard, F., Klinger, Y., Doin, M.-P., 2014. The Burst-Like Behavior of Aseismic Slip on a Rough Fault: The Creeping Section of the Haiyuan Fault, China. *Bull. Seismol. Soc. Am.* 105, 480–488. doi:10.1785/0120140237

Jones, R.R., Holdsworth, R.E., 1998. Oblique simple shear in transpression zones. *Geol. Soc. London, Spec. Publ.* 135, 35–40. doi:10.1144/GSL.SP.1998.135.01.03

Kirschner, D.L., Teixell, a., 1996. Three-dimensional geometry of kink bands in slates and its relationship with finite strain. *Tectonophysics* 262, 195–211. doi:10.1016/0040-1951(96)00003-0

Kisters, A.F.M., Kolb, J., Meyer, F.M., 1998. Gold mineralization in high-grade metamorphic shear zones of the Renco Mine, southern Zimbabwe. *Econ. Geol.* 93, 587–601. doi:10.2113/gsecongeo.93.5.587

Kisters, A.F., Kolb, J., Meyer, F.M., Hoernes, S., 2000. Hydrologic segmentation of high-temperature shear zones: structural, geochemical and isotopic evidence from auriferous mylonites of the Renco mine, Zimbabwe. *J. Struct. Geol.* 22, 811–829. doi:10.1016/S0191-8141(00)00006-7

Kokelaar, P., 1988. Tectonic controls of Ordovician arc and marginal basin volcanism in Wales. *J. Geol. Soc. London.* 145, 759–775. doi:10.1144/gsjgs.145.5.0759

Kolb, J., Kisters, A., Hoernes, S., Meyer, F., 2000. The origin of fluids and nature of fluid–rock interaction in mid-crustal auriferous mylonites of the Renco mine, southern Zimbabwe. *Miner. Depos.* 35, 109–125.

Krantz, R.W., 1988. Multiple fault sets and three-dimensional strain: Theory and application. *J. Struct. Geol.* 10, 225–237. doi:10.1016/0191-8141(88)90056-9

Kruckenberger, S.C., Ferré, E.C., Teyssier, C., Vanderhaeghe, O., Whitney, D.L., Seaton, N.C.A., Skord, J.A., 2010. Viscoplastic flow in migmatites deduced from fabric anisotropy: An example from the Naxos dome, Greece. *J. Geophys. Res. Solid Earth* 115, n/a-n/a.

doi:10.1029/2009JB007012

- 1 Laing, W.P., 2004. Tension vein arrays in progressive strain: complex but predictable architecture,  
2 and major hosts of ore deposits. *J. Struct. Geol.* 26, 1303–1315. doi:10.1016/j.jsg.2003.11.006  
3  
4  
5 Lawn, B., 1993. *Fracture of Brittle Solids*, Cambridge Music Handbooks. Cambridge University  
6 Press.  
7  
8  
9 Lester, D.R., Ord, A., Hobbs, B.E., 2012. The mechanics of hydrothermal systems: II. Fluid mixing  
10 and chemical reactions. *Ore Geol. Rev.* 49, 45–71. doi:10.1016/j.oregeorev.2012.08.002  
11  
12  
13 Liesa, C.L., Lisle, R.J., 2004. Reliability of methods to separate stress tensors from heterogeneous  
14 fault-slip data. *J. Struct. Geol.* 26, 559–572. doi:10.1016/j.jsg.2003.08.010  
15  
16  
17 Lin, A., 2001a. S–C fabrics developed in cataclastic rocks from the Nojima fault zone, Japan and  
18 their implications for tectonic history. *J. Struct. Geol.* 23, 1167–1178. doi:10.1016/S0191-  
19 8141(00)00171-1  
20  
21  
22  
23 Lin, S., 2001b. Stratigraphic and structural setting of the Hemlo gold deposit, Ontario, Canada.  
24 *Econ. Geol.* 96, 477–507.  
25  
26  
27 Lin, S., Jiang, D., Williams, P.F., 1998. Transpression (or transtension) zones of triclinic symmetry:  
28 natural example and theoretical modelling. *Geol. Soc. London, Spec. Publ.* 135, 41–57.  
29 doi:10.1144/GSL.SP.1998.135.01.04  
30  
31  
32  
33 Lisle, R.J., 1988. ROMSA : A BASIC P R O G R A M FOR PALEOSTRESS ANALYSIS USING  
34 FAULT-STRIATION DATA. *Comput. Geosci.* 14, 255–259.  
35  
36  
37  
38 Lisle, R.J., Vandycke, S., 1996. Separation of multiple stress events by fault striation analysis: an  
39 example from Variscan and younger structures at Ogmores, South Wales. *J. Geol. Soc. London.*  
40 153, 945–953. doi:10.1144/gsjgs.153.6.0945  
41  
42  
43  
44 Lisle, R.J., Orife, T., 2002. STRESSTAT: a Basic program for numerical evaluation of multiple  
45 stress inversion results. *Comput. Geosci.* 28, 1037–1040. doi:10.1016/S0098-3004(02)00018-3  
46  
47  
48 Lisle, R.J., Orife, T.O., Arlegui, L., Liesa, C., Srivastava, D.C., 2006. Favoured states of  
49 palaeostress in the Earth's crust: evidence from fault-slip data. *J. Struct. Geol.* 28, 1051–1066.  
50 doi:10.1016/j.jsg.2006.03.012  
51  
52  
53  
54 Manning, C.E., Ingebritsen, S.E., 1999. Permeability of the Continental Crust: Implications of  
55 Geothermal Data and Metamorphic Systems. *Rev. Geophys.* 37, 127–150.  
56  
57  
58 Marjoribanks, R., 2010. Geological methods in mineral exploration and mining, *Geological*  
59 *Methods in Mineral Exploration and Mining.* doi:10.1007/978-3-540-74375-0  
60  
61  
62  
63  
64  
65

- 1  
2  
3  
4  
5  
6  
7  
8  
9  
10  
11  
12  
13  
14  
15  
16  
17  
18  
19  
20  
21  
22  
23  
24  
25  
26  
27  
28  
29  
30  
31  
32  
33  
34  
35  
36  
37  
38  
39  
40  
41  
42  
43  
44  
45  
46  
47  
48  
49  
50  
51  
52  
53  
54  
55  
56  
57  
58  
59  
60  
61  
62  
63  
64  
65
- Marrett, R., Allmendinger, R.W., 1990. Kinematic analysis of fault-slip data. *J. Struct. Geol.* 12, 973–986. doi:[http://dx.doi.org/10.1016/0191-8141\(90\)90093-E](http://dx.doi.org/10.1016/0191-8141(90)90093-E)
- McCuaig, T.C., Hronsky, J.M.A., 2016. The mineral system concept: the key to exploration targeting. *Econ. Geol.* 153–175.
- Mclellan, J.G., Blenkinsop, T., Nugus, M., Erickson, M., 2007. Numerical simulation of deformation and controls on mineralization at the Sunrise Dam Gold Mine, Western Australia, in: *Proceedings of the Ninth Biennial SGA Meeting*. pp. 1455–1458.
- Micklethwaite, S., Cox, S.F., 2004. Fault-segment rupture, aftershock-zone fluid flow, and mineralization. *Geology* 32, 813. doi:[10.1130/G20559.1](https://doi.org/10.1130/G20559.1)
- Micklethwaite, S., Cox, S., 2006. Progressive fault triggering and fluid flow in aftershock domains: Examples from mineralized Archaean fault systems. *Earth Planet. Sci. Lett.* 250, 318–330. doi:[10.1016/j.epsl.2006.07.050](https://doi.org/10.1016/j.epsl.2006.07.050)
- Micklethwaite, S., Ford, A., Witt, W., Sheldon, H.A., 2015. The where and how of faults, fluids and permeability - insights from fault stepovers, scaling properties and gold mineralisation. *Geofluids* 15, 240–251. doi:[10.1111/gfl.12102](https://doi.org/10.1111/gfl.12102)
- Miller, J.M., Wilson, C.J.L., 2004a. Structural analysis of faults related to a heterogeneous stress history: reconstruction of a dismembered gold deposit, Stawell, western Lachlan Fold Belt, Australia. *J. Struct. Geol.* 26, 1231–1256. doi:[10.1016/j.jsg.2003.11.004](https://doi.org/10.1016/j.jsg.2003.11.004)
- Miller, J.M., Wilson, C.J.L., 2004b. Structural analysis of faults related to a heterogeneous stress history: reconstruction of a dismembered gold deposit, Stawell, western Lachlan Fold Belt, Australia. *J. Struct. Geol.* 26, 1231–1256. doi:[10.1016/j.jsg.2003.11.004](https://doi.org/10.1016/j.jsg.2003.11.004)
- Miller, J., Blewett, R., Tunjic, J., Connors, K., 2010. The role of early formed structures on the development of the world class St Ives Goldfield, Yilgarn, WA. *Precambrian Res.* 183, 292–315. doi:[10.1016/j.precamres.2010.08.002](https://doi.org/10.1016/j.precamres.2010.08.002)
- Mitchell, T.M., Faulkner, D.R., 2008. Experimental measurements of permeability evolution during triaxial compression of initially intact crystalline rocks and implications for fluid flow in fault zones. *J. Geophys. Res. Solid Earth* 113, 1–16. doi:[10.1029/2008JB005588](https://doi.org/10.1029/2008JB005588)
- Mitra, G., 1979. Ductile deformation zones in Blue Ridge basement rocks and estimation of finite strains. *Geol. Soc. Am. Bull.* 90, 935–951. doi:[10.1130/0016-7606\(1979\)90<935:DDZIBR>2.0.CO;2](https://doi.org/10.1130/0016-7606(1979)90<935:DDZIBR>2.0.CO;2)
- Moeck, I., Kwiatek, G., Zimmermann, G., 2009. Slip tendency analysis, fault reactivation potential and induced seismicity in a deep geothermal reservoir. *J. Struct. Geol.* 31, 1174–1182.



- 1 Morelli, R.M., Creaser, R.A., Selby, D., Kontak, D.J., Horne, R.J., 2005. Rhenium-Osmium  
2 Geochronology of Arsenopyrite in Meguma Group Gold Deposits, Meguma Terrane, Nova  
3 Scotia, Canada: Evidence for Multiple Gold-Mineralizing Events Economic Geol., 1229–1242.  
4  
5  
6  
7 Morelli, R.M., Bell, C.C., Creaser, R.A., Simonetti, A., 2010. Constraints on the genesis of gold  
8 mineralization at the Homestake Gold Deposit, Black Hills, South Dakota from rhenium-  
9 osmium sulfide geochronology. *Miner. Depos.* 45, 461–480. doi:10.1007/s00126-010-0284-9  
10  
11  
12  
13 Morey, A.A., Weinberg, R.F., Bierlein, F.P., 2007. The structural controls of gold mineralisation  
14 within the Bardoc Tectonic Zone, Eastern Goldfields Province, Western Australia:  
15 Implications for gold endowment in shear systems. *Miner. Depos.* 42, 583–600.  
16  
17  
18  
19  
20  
21  
22  
23  
24  
25  
26  
27  
28  
29  
30  
31  
32  
33  
34  
35  
36  
37  
38  
39  
40  
41  
42  
43  
44  
45  
46  
47  
48  
49  
50  
51  
52  
53  
54  
55  
56  
57  
58  
59  
60  
61  
62  
63  
64  
65
- Morris, A.P., Ferrill, D. a., 2009. The importance of the effective intermediate principal stress ( $\sigma_2$ ) to fault slip patterns. *J. Struct. Geol.* 31, 950–959. doi:10.1016/j.jsg.2008.03.013
- Morris, A., Ferrill, D.A., Henderson, D.B., 1996. Slip-tendency analysis and fault reactivation 275–278.
- Munyai, M.R., Charlesworth, E.G., Dirks, P.H.G.M., 2011. Archaean gold mineralisation during post-orogenic extension in the New Consort Gold Mine, Barberton Greenstone Belt, South Africa. *South African J. Geol.* 114, 121–144.
- Mutemeri, N., 2001. Fluids and gold mineralization at Arcturus mine, Zimbabwe. Zimbabwe.
- Nugus, M.J., Blenkinsop, T.G., Dominy, S.C., Robson, S., 2003. Enigmatic kinematics resolved in the Taurus Shear Zone Golden Pig Gold mine, Southern Cross, Western Australia - resource implications., in: *Proceedings of the 5th International Mining Geology Conference*. Bendigo, pp. 171–179.
- Oertel, G., 1965. The mechanism of faulting in clay experiments. *Tectonophysics* 2, 343–393. doi:10.1016/0040-1951(65)90032-6
- Oesterlen, P., Blenkinsop, T., 1994. Extension directions and strain near the failed triple junction of the Zambezi and Luangwa Rift zones, southern Africa. *J. African Earth Sci.* 18, 175–180.
- Oliver, N.H.S., Bons, P.D., 2001. Mechanisms of fluid flow and fluid-rock interaction in fossil metamorphic hydrothermal systems inferred from vein-wallrock patterns, geometry and microstructure. *Geofluids* 1, 137–162. doi:10.1046/j.1468-8123.2001.00013.x
- Oliver, N.H.S., Thomson, B., Freitas-silva, F.H., Holcombe, R.J., Rusk, B., Almeida, B.S., Faure, K., Davidson, G.R., Esper, E.L., Guimarães, P.J., Dardenne, M.A., 2015. Local and Regional

Mass Transfer During Thrusting , Veining , and Boudinage in the Genesis of the Giant Shale-Hosted Paracatu Gold Deposit , Minas Gerais , Brazil. *Econ. Geol.* 110, 1803–1834.

- 1  
2  
3 Ord, A., Hunt, G.W., Hobbs, B.E., 2010. Patterns in our planet: defining new concepts for the  
4 application of multi-scale non-equilibrium thermodynamics to Earth-system science. *Philos.*  
5  
6  
7 Ord, A., Hobbs, B.E., Lester, D.R., 2012. The mechanics of hydrothermal systems: I. Ore systems  
8 as chemical reactors. *Ore Geol. Rev.* 49, 1–44. doi:10.1016/j.oregeorev.2012.08.003  
9  
10  
11 Ord, A., Munroe, M., Hobbs, B.E., 2016. Hydrothermal mineralising systems as chemical reactors.  
12 *Ore Geol. Rev.* 79, 155–179.  
13  
14  
15 Peng, Z., Gomberg, J., 2010. An integrated perspective of the continuum between earthquakes and  
16 slow-slip phenomena. *Nat. Geosci.* 3, 599–607. doi:10.1038/ngeo940  
17  
18  
19  
20 Phillips, G.N., Groves, D.I., 1983. The nature of Archaean gold-bearing fluids as deduced from  
21 gold deposits of Western Australia. *J. Geol. Soc. Aust.* 30, 25–39.  
22 doi:10.1080/00167618308729234  
23  
24  
25  
26 Phillips, G.N., Powell, R., 2015. A practical classification of gold deposits, with a theoretical basis.  
27 *Ore Geol. Rev.* 65, 568–573. doi:10.1016/j.oregeorev.2014.04.006  
28  
29  
30  
31 Pitcairn, I.K., Teagle, D.A.H., Craw, D., Olivo, G.R., Kerrich, R., Brewer, T.S., 2006. Sources of  
32 metals and fluids in orogenic gold deposits: Insights from the Otago and Alpine schists, New  
33 Zealand. *Econ. Geol.* 101, 1525–1546. doi:10.2113/gsecongeo.101.8.1525  
34  
35  
36  
37 Platt, J.P., Vissers, R.L.M., 1989. Extensional collapse of thickened continental lithosphere: A  
38 working hypothesis for the Alboran Sea and Gibraltar Arc. *Geology* 17, 540–543.  
39  
40  
41 Platten, I.M., Dominy, S.C., 1999. Re-evaluation of quartz vein history in the dolgellau gold-belt  
42 North Wales, United Kingdom. *Geol. J.* 34, 369–391. doi:10.1002/(SICI)1099-  
43 1034(199911/12)34:4<369::AID-GJ832>3.0.CO;2-G  
44  
45  
46  
47 Platten, I.M., Dominy, S.C., 2009. Geological mapping in the evaluation of structurally controlled  
48 gold veins: a case study from the Dolgellau gold-belt, north Wales, UK, in: *Proc. Conf. World*  
49 *Gold.* pp. 151–166.  
50  
51  
52  
53 Potma, W., Roberts, P.A., Schaub, P.M., Sheldon, H.A., Zhang, Y., Hobbs, B.E., Ord, A., 2008.  
54 Predictive targeting in Australian orogenic-gold systems at the deposit to district scale using  
55 numerical modelling. *Aust. J. Earth Sci.* 55, 101–122. doi:Doi 10.1080/08120090701673328  
56  
57  
58  
59 Potts, G.J., Reddy, S.M., 2000. Application of younging tables to the construction of relative  
60 deformation histories—1: Fracture systems. *J. Struct. Geol.* 22, 1473–1490.  
61  
62  
63  
64  
65

doi:10.1016/S0191-8141(00)00044-4

- 1 Poulsen, K.H., 1996. Lode gold, in: Eckstrand, O.R., Sinclair, W.D., Thorpe, R.I. (Eds.), The  
2 Geology of North America. Geological Society of America, pp. 323–328.  
3  
4  
5 Poulsen, H., Robert, F., 1989. Shear zones and gold: Practical examples from the southern Canadian  
6 Shield, in: Bursnall, J.T. (Ed.), Mineralization and Shear Zones, Geological Association of  
7 Canada, Short Course Notes 6. Montreal, pp. 239–266.  
8  
9  
10 Poulsen, K.H., Robert, F., Dube, B., 2000. Geological classification of Canadian gold deposits,  
11 Bulletin of the Geological Survey of Canada. doi:10.1126/science.ns-6.149S.521-a  
12  
13  
14  
15 Raine, M.D., 2005. Polyphase deformation and the structural controls on economic gold occurrences  
16 within the Bendigo gold field, central Victoria, Australia. James Cook University.  
17  
18  
19 Ramsay, J.G., Graham, R.H., 1970. Strain variation in shear belts. *Can. J. Earth Sci.* 7, 786–813.  
20  
21 doi:10.1139/e70-078  
22  
23  
24 Reches, Z., 1983. Faulting of rocks in three-dimensional strain fields II. Theoretical analysis.  
25 *Tectonophysics* 95, 133–156. doi:http://dx.doi.org/10.1016/0040-1951(83)90264-0  
26  
27  
28 Ridley, J., 1993. The relations between mean rock stress and fluid flow in the crust: With reference  
29 to vein- and lode-style gold deposits. *Ore Geol. Rev.* 8, 23–37. doi:10.1016/0169-  
30 1368(93)90026-U  
31  
32  
33  
34 Riley, M.S., 2005. Fracture trace length and number distributions from fracture mapping. *J.*  
35 *Geophys. Res. B Solid Earth* 110, 1–16. doi:10.1029/2004JB003164  
36  
37  
38 Robert, F., Boullier, A.-M., Firdaous, K., 1995. Gold-quartz veins in metamorphic terranes and  
39 their bearing on the role of fluids in faulting. *J. Geophys. Res. Solid Earth* 100, 12861–12879.  
40  
41 doi:10.1029/95JB00190  
42  
43  
44 Royden, L.H., 1993. The tectonic expression of slab pull at continental convergent boundaries.  
45 *Tectonics* 12, 303–325.  
46  
47  
48 Rutter, E.H., 1986. On the nomenclature of mode of failure transitions in rocks. *Tectonophysics*  
49 122, 381–387. doi:10.1016/0040-1951(86)90153-8  
50  
51  
52 Sanderson, D.J., Marchini, W.R.D., 1984. Transpression. *J. Struct. Geol.* 6, 449–458.  
53  
54 doi:http://dx.doi.org/10.1016/0191-8141(84)90058-0  
55  
56  
57 Sanderson, D.J., Nixon, C.W., 2015. The use of topology in fracture network characterization. *J.*  
58 *Struct. Geol.* 72, 55–66. doi:10.1016/j.jsg.2015.01.005  
59  
60  
61 Sanislav, I. V., Kolling, S.L., Brayshaw, M., Cook, Y.A., Dirks, P.H.G.M., Blenkinsop, T.G.,  
62  
63  
64  
65

1 Mturi, M.I., Ruhega, R., 2015. The geology of the giant Nyankanga gold deposit, Geita  
2 Greenstone Belt, Tanzania. *Ore Geol. Rev.* 69, 1–16. doi:10.1016/j.oregeorev.2015.02.002

3 Sanislav, I. V., Brayshaw, M., Kolling, S.L., Dirks, P.H.G.M., Cook, Y.A., Blenkinsop, T.G., 2017.  
4 The structural history and mineralization controls of the world-class Geita Hill gold deposit,  
5 Geita Greenstone Belt, Tanzania. *Miner. Depos.* 52, 257–279. doi:10.1007/s00126-016-0660-1

6  
7  
8  
9 Schaub, P.M., Zhao, C., 2002. Numerical models of gold-deposit formation in the Bendigo–  
10 Ballarat Zone, Victoria. *Aust. J. Earth Sci.* 49, 1077–1096. doi:10.1046/j.1440-  
11 0952.2002.00964.x

12  
13  
14 Schaub, P.M., Rawling, T.J., Dugdale, L.J., Wilson, C.J.L., 2006. Factors controlling the location  
15 of gold mineralisation around basalt domes in the stawell corridor: insights from coupled 3D  
16 deformation – fluid-flow numerical models. *Aust. J. Earth Sci.* 53, 841–862.  
17  
18 doi:10.1080/08120090600827496

19  
20  
21  
22 Shan, Y., Fry, N., 2005. A hierarchical cluster approach for forward separation of heterogeneous  
23 fault/slip data into subsets. *J. Struct. Geol.* 27, 929–936. doi:10.1016/j.jsg.2005.02.001

24  
25  
26 Sheldon, H.A., Micklethwaite, S., 2007. Damage and permeability around faults: Implications for  
27 mineralization. *Geology* 35, 903. doi:10.1130/G23860A.1

28  
29  
30  
31 Shepherd, T.J., Allen, P.M., 1985. Metallogenesis in the Harlech Dome, North Wales: A fluid  
32 inclusion interpretation. *Miner. Depos.* 20, 159–168. doi:10.1007/BF00204560

33  
34  
35  
36  
37  
38  
39  
40 Shepherd, T.J., Bottrell, S.H., Miller, M.F., 1991. Fluid inclusion volatiles as an exploration guide  
41 to black shale-hosted gold deposits, Dolgellau gold belt, North Wales, UK. *J. Geochemical*  
42  
43  
44  
45  
46  
47  
48  
49  
50  
51  
52  
53  
54  
55  
56  
57  
58  
59  
60  
61  
62  
63  
64  
65

Sibson, R., 1985. A note on fault reactivation. *J. Struct. Geol.* 7, 3–6.

Sibson, R., 1987. Earthquake rupturing as a mineralizing agent in hydrothermal systems. *Geology* 15, 710–704.

Sibson, R.H., Robert, F., Poulsen, K.H., 1988. High-angle reverse faults, fluid-pressure cycling, and mesothermal gold-quartz deposits. *Geology* 16, 551–555. doi:10.1130/0091-7613(1988)016<0551:HARFFP>2.3.CO;2

Smith, D.L., Evans, B., 1984. Diffusional crack healing in quartz. *J. Geophys. Res. Solid Earth* 89, 4125–4135. doi:10.1029/JB089iB06p04125

Stauffer, D., Aharony, A., 1994. *Introduction To Percolation Theory*. Taylor & Francis.

Stephens, J.R., Mair, J.L., Oliver, N.H., Hart, C.J., Baker, T., 2004. *Structural and mechanical*

controls on intrusion-related deposits of the Tombstone Gold Belt, Yukon, Canada, with comparisons to other vein-hosted ore-deposit types. *J. Struct. Geol.* 26, 1025–1041.  
doi:10.1016/j.jsg.2003.11.008

Stillwell, F.L., 1918. Replacement in the Bendigo quartz veins and its relation to gold deposition. *Econ. Geol.* 13, 100–111.

Sun, X., Zhang, Y., Xiong, D., Sun, W., Shi, G., Zhai, W., Wang, S., 2009. Crust and mantle contributions to gold-forming process at the Daping deposit, Ailaoshan gold belt, Yunnan, China. *Ore Geol. Rev.* 36, 235–249. doi:10.1016/j.oregeorev.2009.05.002

Sung, Y.-H., Ciobanu, C.L., Pring, a., Brügger, J., Skinner, W., Cook, N.J., Nugus, M., 2007. Tellurides from Sunrise Dam gold deposit, Yilgarn Craton, Western Australia: a new occurrence of nagyágite. *Mineral. Petrol.* 91, 249–270. doi:10.1007/s00710-007-0199-z

Tenthorey, E., Cox, S.F., Todd, H.F., 2003. Evolution of strength recovery and permeability during fluid–rock reaction in experimental fault zones. *Earth Planet. Sci. Lett.* 206, 161–172.  
doi:10.1016/S0012-821X(02)01082-8

Thakur, P., Srivastava, D.C., Gupta, P.K., 2017. The genetic algorithm : A robust method for stress inversion. *J. Struct. Geol.* 94, 227–239. doi:10.1016/j.jsg.2016.11.015

Thiele, S.T., Jessell, M.W., Lindsay, M., Ogarko, V., Wellmann, J.F., Pakyuz-Charrier, E., 2016a. The topology of geology 1: Topological analysis. *J. Struct. Geol.* 91, 27–38.  
doi:10.1016/j.jsg.2016.08.009

Thiele, S.T., Jessell, M.W., Lindsay, M., Wellmann, J.F., Pakyuz-Charrier, E., 2016b. The topology of geology 2: Topological uncertainty. *J. Struct. Geol.* 91, 74–87.  
doi:10.1016/j.jsg.2016.08.010

Tikoff, B., Fossen, H., 1993. Simultaneous pure and simple shear: the unifying deformation matrix. *Tectonophysics* 217, 267–283.

Tikoff, B., Greene, D., 1997. Stretching lineations in transpressional shear zones: an example from the Sierra Nevada Batholith, California. *J. Struct. Geol.* 19, 29–39.

Tikoff, B., Fossen, H., 1999. Three-dimensional reference deformations and strain facies. *J. Struct. Geol.* 21, 1497–1512. doi:10.1016/S0191-8141(99)00085-1

Tikoff, B., Blenkinsop, T., Kruckenberg, S.C., Morgan, S., Newman, J., Wojtal, S., 2013. A perspective on the emergence of modern structural geology: Celebrating the feedbacks between historical-based and process-based approaches. *Web Geol. Sci. Adv. Impacts Interact. Special Pa*, 65–119. doi:doi:10.1130/2013.2500(03)

- 1  
2  
3  
4  
5  
6  
7  
8  
9  
10  
11  
12  
13  
14  
15  
16  
17  
18  
19  
20  
21  
22  
23  
24  
25  
26  
27  
28  
29  
30  
31  
32  
33  
34  
35  
36  
37  
38  
39  
40  
41  
42  
43  
44  
45  
46  
47  
48  
49  
50  
51  
52  
53  
54  
55  
56  
57  
58  
59  
60  
61  
62  
63  
64  
65
- Townend, J., Zoback, M.D., 2000. How faulting keeps the crust strong. *Geology* 28, 399–402.  
doi:10.1130/0091-7613(2000)28<399:HFKTCS>2.0.CO;2
- Tripp, G.I., Vearncombe, J.R., 2004. Fault/fracture density and mineralization: A contouring method for targeting in gold exploration. *J. Struct. Geol.* 26, 1087–1108.  
doi:10.1016/j.jsg.2003.11.002
- Tunks, A.J., Selley, D., Rogers, J.R., Brabham, G., 2004. Vein mineralization at the Damang Gold Mine, Ghana: controls on mineralization. *J. Struct. Geol.* 26, 1257–1273.  
doi:10.1016/j.jsg.2003.11.005
- Twiss, R.J., Moores, E.M., 2007. *Structural Geology*, 2nd Editio. ed. W.H. Freeman.
- Underhill, J.R., Woodcock, N.H., 1987. Faulting mechanisms in high-porosity sandstones; New Red Sandstone, Arran, Scotland. *Geol. Soc. London, Spec. Publ.* 29, 91–105.  
doi:10.1144/GSL.SP.1987.029.01.09
- Van der Pluijm, B.A., Marshak, S., 2004. *Earth Structure: An Introduction to Structural Geology and Tectonics*. W.W. Norton.
- van Ryt, M.R., Sanislav, I. V., Dirks, P.H.G.M., Huizenga, J.M., Mturi, M.I., Kolling, S.L., 2017. Alteration paragenesis and the timing of mineralised quartz veins at the world-class Geita Hill gold deposit, Geita Greenstone Belt, Tanzania. *Ore Geol. Rev.* 0–1.  
doi:10.1016/j.oregeorev.2017.08.023
- Vearncombe, J.R., 1998. Shear zones, fault networks, and Archean gold. *Geology* 26, 855.  
doi:10.1130/0091-7613(1998)026<0855:SZFNAA>2.3.CO;2
- Vearncombe, J., Vearncombe, S., 1998. Structural data from drill core. *Aust. Inst. Geosci. Bull.* 22, 67–82.
- Vearncombe, J., Zelic, M., 2015. Structural paradigms for gold: do they help us find and mine? *Appl. Earth Sci.* 124. doi:10.1179/1743275815Y.0000000003
- Warren, J.D., Thébaud, N., Miller, J.M., Micklethwaite, S., 2015. Distinguishing between local versus regional extension as a control on orogenic gold mineralisation: The new 2.4Moz Castle Hill Camp, WA. *Precambrian Res.* 269, 242–260. doi:10.1016/j.precamres.2015.08.008
- Weinberg, R.F., van der Borgh, P., 2008. Extension and gold mineralization in the Archean Kalgoorlie Terrane, Yilgarn Craton. *Precambrian Res.* 161, 77–88.
- Weinberg, R.F., Hodkiewicz, P.F., Groves, D.I., 2004. What controls gold distribution in Archean terranes? *Geology* 32, 545. doi:10.1130/G20475.1

- 1  
2  
3  
4  
5  
6  
7  
8  
9  
10  
11  
12  
13  
14  
15  
16  
17  
18  
19  
20  
21  
22  
23  
24  
25  
26  
27  
28  
29  
30  
31  
32  
33  
34  
35  
36  
37  
38  
39  
40  
41  
42  
43  
44  
45  
46  
47  
48  
49  
50  
51  
52  
53  
54  
55  
56  
57  
58  
59  
60  
61  
62  
63  
64  
65
- Weiss, L. e., McIntyre, D.B., 1957. Structural geometry of Dalradian rocks at Loch Leven, Scottish Highlands. *J. Geol.* 65, 575–602.
- Witt, W., Vanderhor, F., 1998. Diversity within a unified model for Archaean gold mineralization in the Yilgarn Craton of Western Australia: An overview of the late-orogenic, structurally-controlled gold deposits. *Ore Geol. Rev.* 13, 29–64. doi:10.1016/S0169-1368(97)00013-9
- Woodcock, N.H., Underhill, J.R., 1987. Emplacement-related fault patterns around the Northern Granite, Arran, Scotland. *Geol. Soc. Am. Bull.* 98, 515–527. doi:10.1130/0016-7606(1987)98<515:EFPATN>2.0.CO;2
- Wyman, D.A., Cassidy, K.F., Hollings, P., 2016. Orogenic gold and the mineral systems approach: Resolving fact, fiction and fantasy. *Ore Geol. Rev.* 78, 322–335. doi:10.1016/j.oregeorev.2016.04.006
- Wyborn, L.A., Heinrich, C.A., Jaques, A.L., 1994. Australian Proterozoic mineral systems: essential ingredients and mappable criteria, in: *AusIMM Annual Conference, AusIMM Publ. Ser. 5 (94)*, Australian Institute of Mining and Metallurgy, Darwin, pp. 109–115.
- Yamaji, A., Sato, K., Tonai, S., 2010. Stochastic modeling for the stress inversion of vein orientations: Paleostress analysis of Pliocene epithermal veins in southwestern Kyushu, Japan. *J. Struct. Geol.* 32, 1137–1146. doi:10.1016/j.jsg.2010.07.001
- Yardley, B.W.D., 1986. Fluid Migration and Veining in the Connemara Schists, Ireland, in: Walther, J. V, Wood, B.J. (Eds.), *Fluid--Rock Interactions during Metamorphism*. Springer New York, New York, NY, pp. 109–131. doi:10.1007/978-1-4612-4896-5\_5
- Yardley, B.W.D., Cleverley, J.S., 2013. The role of metamorphic fluids in the formation of ore deposits. *Geol. Soc. London, Spec. Publ.* 393, 117–134. doi:10.1144/sp393.5
- Žalohar, J., Vrabec, M., 2007. Paleostress analysis of heterogeneous fault-slip data: The Gauss method. *J. Struct. Geol.* 29, 1798–1810. doi:10.1016/j.jsg.2007.06.009
- Žalohar, J., Vrabec, M., 2008. Combined kinematic and paleostress analysis of fault-slip data: The Multiple-slip method. *J. Struct. Geol.* 30, 1603–1613. doi:10.1016/j.jsg.2008.09.004
- Žalohar, J., Vrabec, M., 2010. Kinematics and dynamics of fault reactivation: The Cosserat approach. *J. Struct. Geol.* 32, 15–27. doi:10.1016/j.jsg.2009.06.008

## Figure Captions

1  
2  
3 Fig. 1. A spectrum of structures that may control hydrothermal mineralization. The top row (A to  
4 D) indicate planar features (mineralization as yellow polygons), the lower row (C to F) show linear  
5 features, emphasized by yellow ellipsoids lines.  
6  
7  
8  
9

10  
11 Fig. 2. Planar deformation structures that may control gold mineralization: Top row shows  
12 individual features, middle row shows deformation zones, and lower row shows networks of zones,  
13 as labeled. The features are arranged within rows from discontinuous on the left to continuous on  
14 the right.  
15  
16  
17  
18  
19  
20

21  
22 Fig. 3. Photographs of deformation zones related to gold mineralization, arranged in order from  
23 discontinuous to continuous deformation at the cm scale. The description of continuity, specified by  
24 scale, avoids ambiguities created by applying the terms “brittle” and “ductile” to these structures.  
25  
26

27  
28 A) Quartz carbonate extensional vein with coarse gold, Sunrise Dam gold mine, formed during D4b  
29 (Table 1). This is an end-member example of discontinuous deformation at a cm scale.  
30

31  
32 B) Breccia from Sunrise Dam Gold Mine consisting of fuchsite-altered host rock fragments with  
33 quartz-carbonate infill, formed during to D4b (Table 1). The breccia is also an example of  
34 discontinuous deformation at a cm scale.  
35  
36

37  
38 C) Quartz carbonate veins and S fabrics (dashed lines), indicating sinistral shear in the center of Star  
39 and Comet pit, Geita Gold Mine, Tanzania. Discontinuous and continuous deformation features  
40 coexist at the cm scale.  
41  
42

43  
44 D) Sunrise Shear zone, open pit, Sunrise Dam Gold Mine, W. Australia. SC fabrics indicate reverse-  
45 sinistral shear during D3 (see Table 1). Discontinuous and continuous deformation features coexist  
46 at the cm scale.  
47  
48

49  
50 E) Penetrative fabric forming zone of dominantly continuous shear at the cm scale, Tropicana gold  
51 deposit, Australia  
52

53  
54 F) Penetrative schistosity and continuous deformation at the m scale, Cornishman open pit,  
55 Southern Cross greenstone belt, W. Australia  
56  
57

58  
59  
60 Fig. 4. Network Topology. Branches connect I, Y and X nodes. NY, NX are numbers of Y and X  
61  
62  
63  
64  
65



nodes respectively. ? indicate an ambiguity in how the three labeled branches can be joined into traces. Which of the upper query larks join to the lower query mark? There is no objective criterion to allow unique traces to be determined. This example is based on an underground exposure of mineralized quartz-carbonate veins in the Astro lode at Sunrise Dam gold mine, W. Australia, which were coeval with mineralization as demonstrated by common alteration and infill assemblages, and by mutually cross-cutting relationships.

Fig. 5. Relationships between syn-mineralization ore bodies (OB), lineations (L) and vorticity vectors (V) in pure shear and simple shear dominated deformation zones. Grey cube indicates undeformed state, black shows deformed state. A) In pure shear dominated zones, V is parallel to L and orebodies also form in this direction. B, C) In Simple-shear dominated zones, L is perpendicular to V. B) Where permeability is created by the L fabric, ore bodies will form in this direction C) where geometrical irregularities and intersecting fabrics (purple planes) occur, ore bodies may form parallel to V.

Fig. 6. Cartoon to show kinematic controls on ore body geometry at Golden Pig mine, Southern Cross greenstone belt, Yilgarn craton, Australia. Lineation and vorticity vector plunge very gently to the South, indicating a pure-shear dominated shear zone. Permeability and/or extension lead to the elongation of ore bodies in this direction. The geometrical controls are similar to Case A in Fig. 5.

Fig. 7. Equal area, lower hemisphere stereoplots of structural elements at Renco, Shamva and Arcturus mines, Zimbabwe craton, showing the variable relationships between ore bodies (black triangles) lineations (black circles) and vorticity vectors (red circles). Great circles are shear planes. All structures have been determined from eigenvector analysis of individual measurements. At Renco and Shamva, lineations are perpendicular to the vorticity vector: simple shear is dominant. At Renco, ore bodies form parallel to lineation because of kinematic and/or fabric controls. Arrow shows reverse movement. At Shamva, ore bodies form perpendicular to lineation and parallel to the vorticity vector, which is also the direction of maximum permeability due to intersections of shears. At Arcturus, lineations are parallel to the vorticity vector (pure shear dominant): ore bodies also form in this direction. Sinistral strike-slip shear characterizes both Shamva and Arcturus.

Fig. 8. Shear zone and fault networks that form in multiple orientations simultaneously. Cubes indicate undeformed state; principal strain axes are parallel to the edges of the white deformed cuboids. A, B: shear zone networks formed in constriction and flattening respectively. C, D: fault

zone networks formed in constriction and flattening respectively. Figure based on Choukroune and Gapais (1983); Krantz (1988); Healy et al. (2015).

1  
2  
3  
4  
5 Fig. 9. Two dimensional Mohr diagrams showing failure conditions for intact rock and failed  
6 surfaces in reactivation. a) The failure envelop for the failed surface has the same coefficient of  
7 internal friction as intact rock, but no cohesion. The optimum surface for reactivation is represented  
8 by an asterisk. Planes represented by any point on the blue sector of the Mohr circle can be  
9 reactivated. Colours show slip tendency from red (high) to green (low) b) The relationship between  
10 planes that can be reactivated and the maximum principal stress for the stress state shown in (a).  
11 Any plane between the two shown can be reactivated. c) The failure envelop for the failed surface  
12 has the same cohesion but a lower coefficient of internal friction. As in (a), surfaces in a range of  
13 possible orientations can be reactivated. d) Reactivation of some planes as only possible for  
14 negative least principal effective stresses: the Mohr circle shown is one example.  
15  
16  
17  
18  
19  
20  
21  
22  
23  
24  
25

26 Fig. 10. Lower hemisphere equal area stereoplots of slip (upper row) and dilation tendencies (lower  
27 row) shown at poles to planes. White numerals show orientations of principal stresses. Diagrams  
28 shown for  $\Phi = (\sigma_2 - \sigma_3)/(\sigma_1 - \sigma_3) = 0, 0.5$  and  $1$ . The red areas of high slip and dilation tendency  
29 show that a variety of orientations can be reactivated for any stress state, and that the pattern  
30 changes as a function of  $\Phi$ .  
31  
32  
33  
34  
35  
36  
37

38 Fig. 11. The open system reactor concept for hydrothermal mineralization, from Ord et al., (2012).  
39 Feedback loops make this system non-linear, and give rise to multifractal properties of mineral  
40 distributions, for example.  
41  
42  
43  
44  
45

46 Fig. 12. Asian Stress States from the World stress map (Heidbach et al., 2008). Stress states are  
47 separated into normal (red), strike-slip (green) and thrust fault (blue). Lines show the azimuth of  
48 maximum horizontal stress. Stress determination methods are shown in the key. In accretionary  
49 orogens (e.g. Sumatra-Indonesian and Philippine arcs), collisional orogens (e.g. the Himalayas) and  
50 intraplate orogens (e.g. the Tian Shan mountains) there are combinations of normal, strike slip and  
51 thrust fault stress states at all depths in the crust.  
52  
53  
54  
55  
56  
57  
58  
59

60 Fig. 13. Workflow for structural analysis of gold deposits  
61  
62  
63  
64  
65

Table 1.

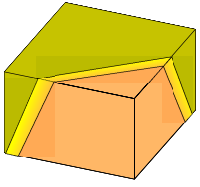
Deformation and intrusive events at Sunrise Dam Gold Mine

- 1
- 2
- 3
- 4
- 5
- 6
- 7
- 8
- 9
- 10
- 11
- 12
- 13
- 14
- 15
- 16
- 17
- 18
- 19
- 20
- 21
- 22
- 23
- 24
- 25
- 26
- 27
- 28
- 29
- 30
- 31
- 32
- 33
- 34
- 35
- 36
- 37
- 38
- 39
- 40
- 41
- 42
- 43
- 44
- 45
- 46
- 47
- 48
- 49
- 50
- 51
- 52
- 53
- 54
- 55
- 56
- 57
- 58
- 59
- 60
- 61
- 62
- 63
- 64
- 65

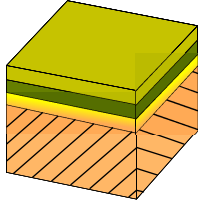
Figure 1

T  
A  
B  
U  
L  
A  
R

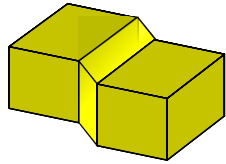
A) Lithological contact



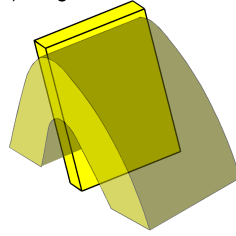
B) Unconformity



C) Deformation zone



D) Hinge surface



E  
L  
O  
N  
G  
A  
T  
E

E) Deformation zones:

Bend

Stepover

Intersection

Damage Zone

F) Boudin Neck

G) Hinge

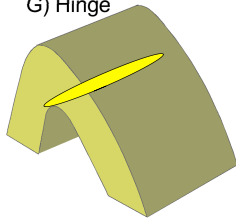
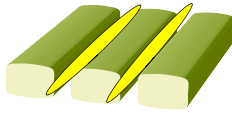
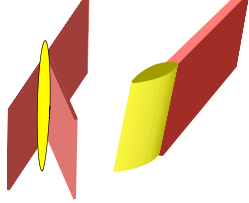
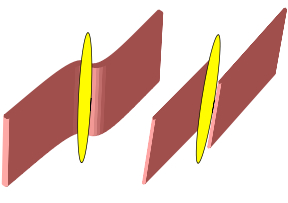
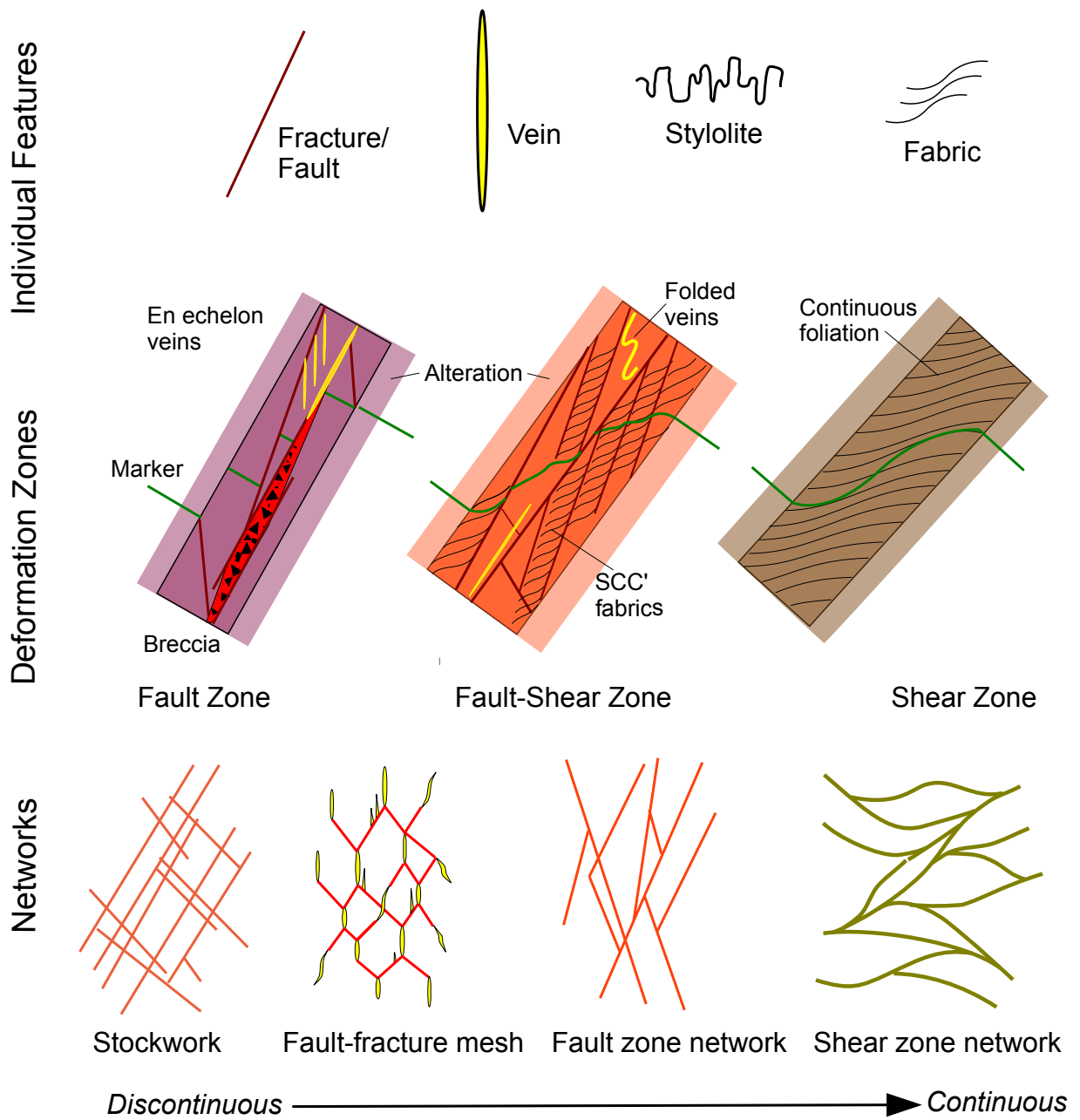
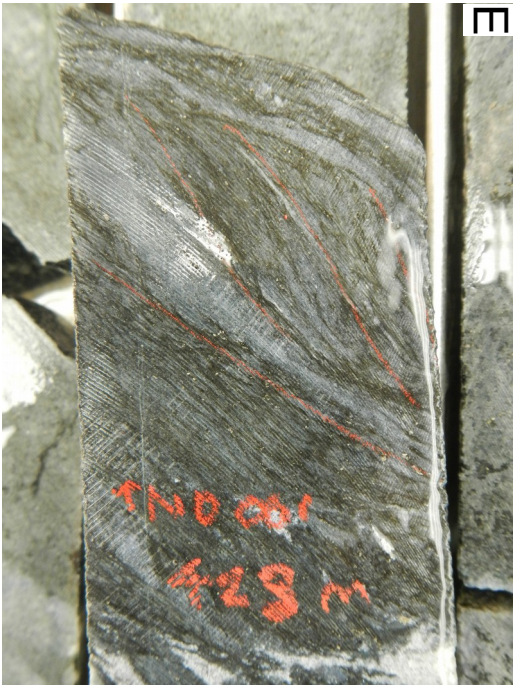


Figure 2





Continuous ←—————→ Discontinuous

Figure 4

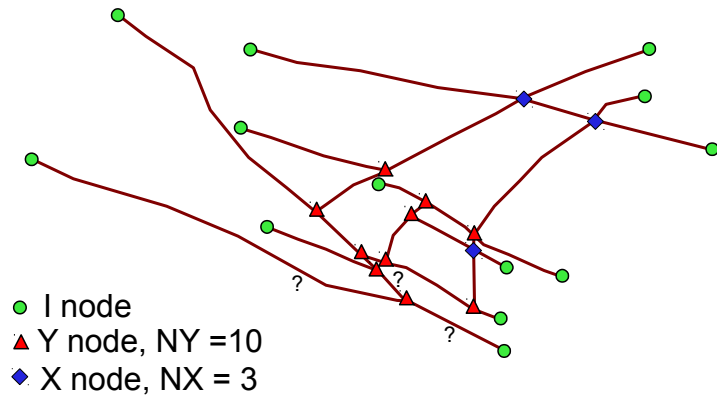


Figure 5

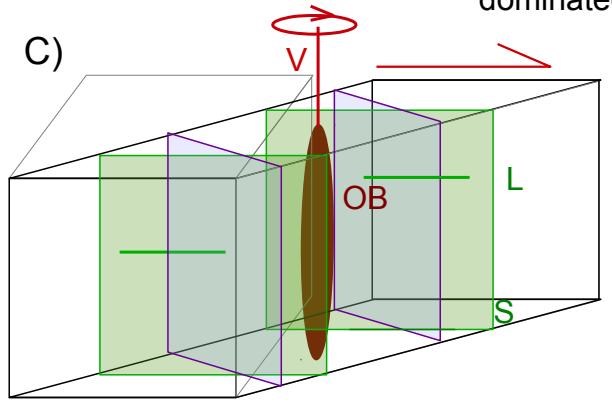
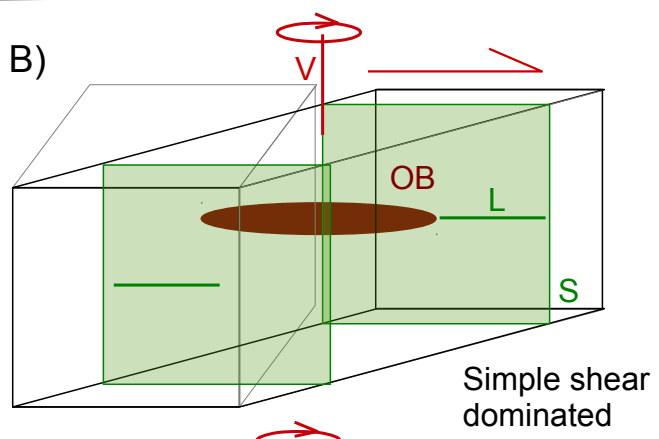
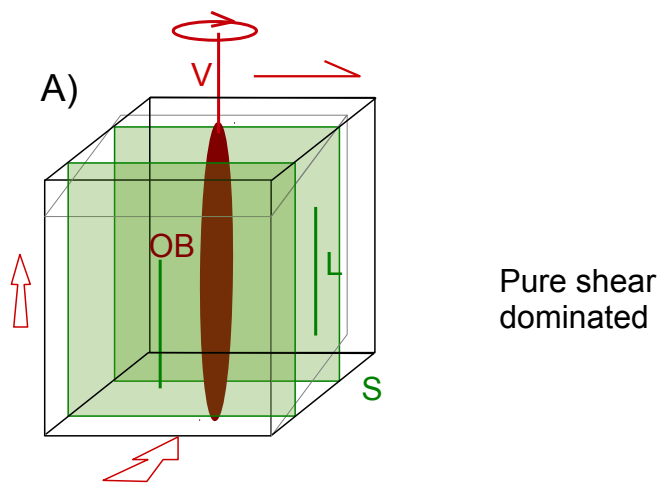




Figure 6

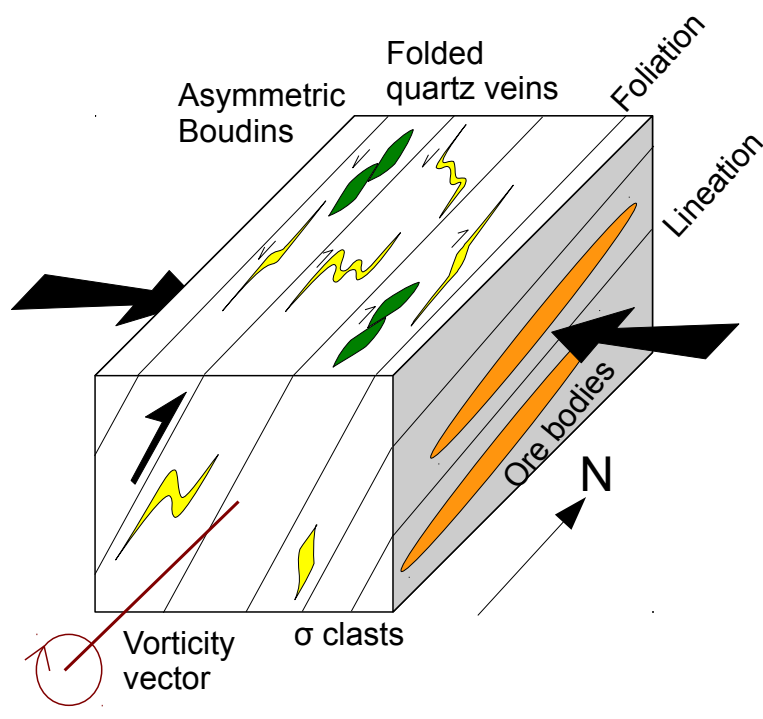


Figure 7

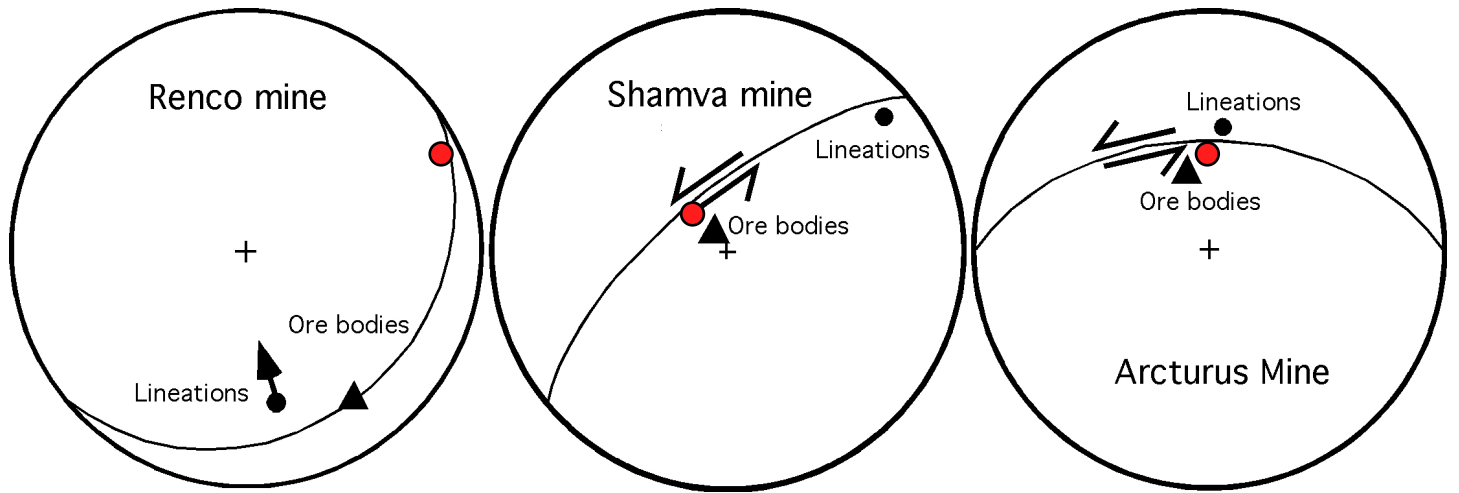
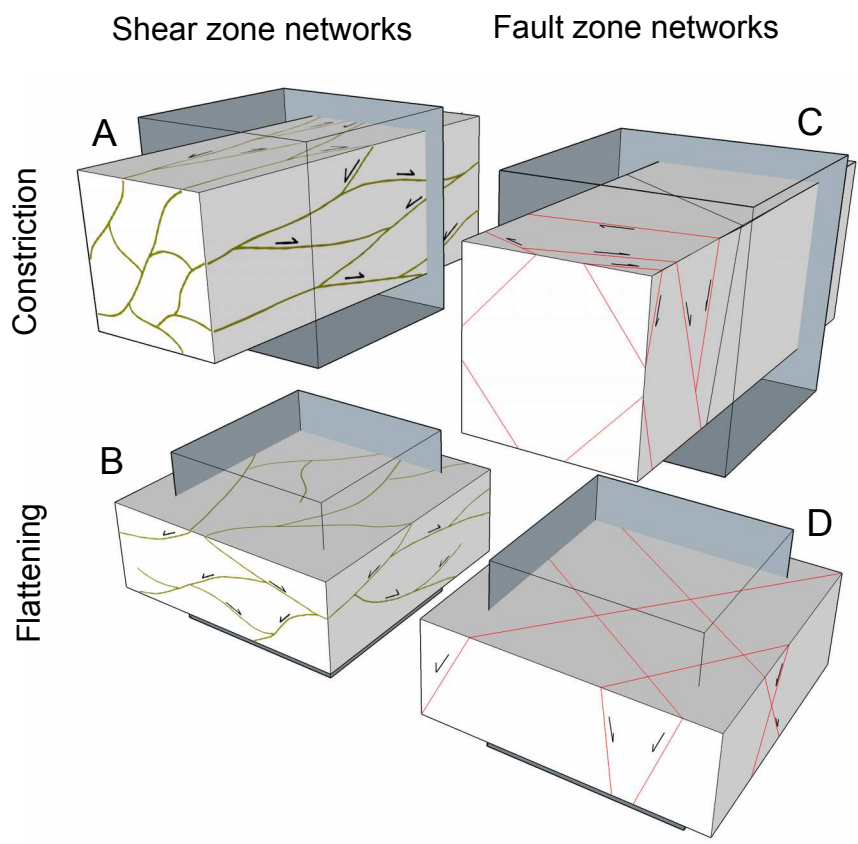


Figure 8



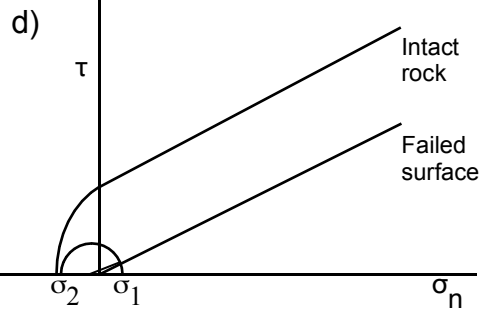
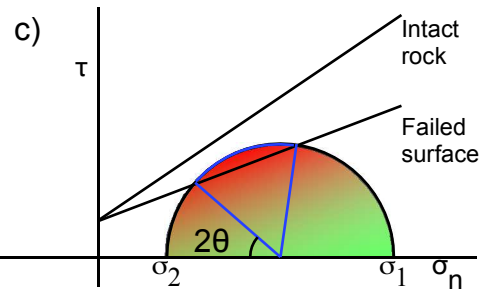
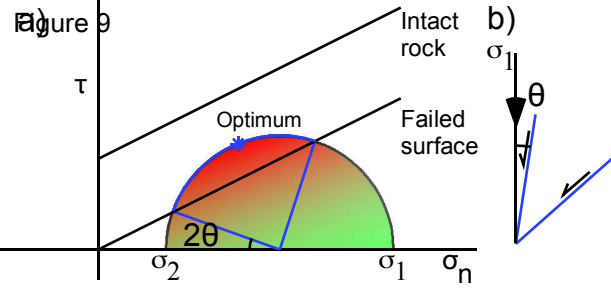
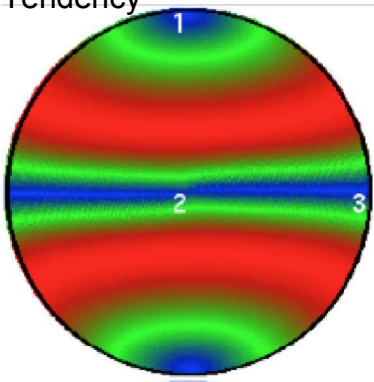
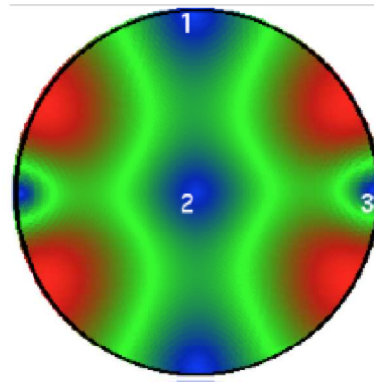


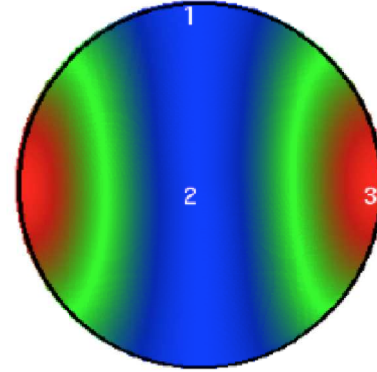
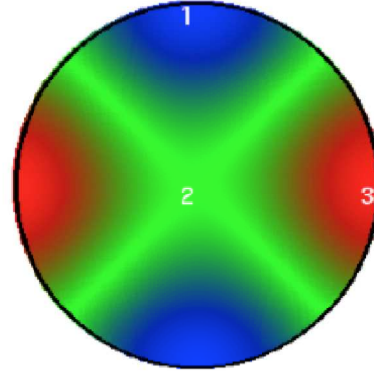
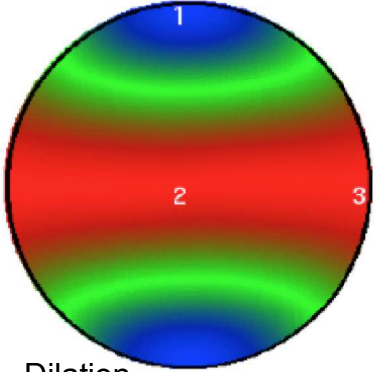
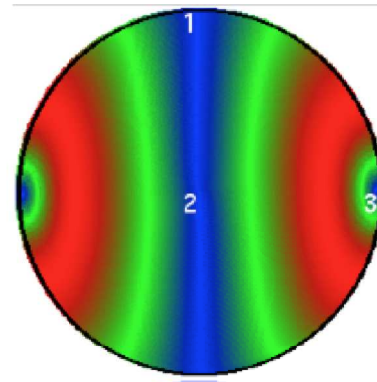
Figure 10  $\phi = 0$   
Tendency



$\phi = 0.5$



$\phi = 1$



Dilation  
Tendency

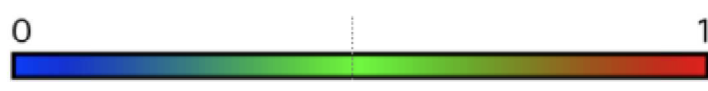


Figure 11

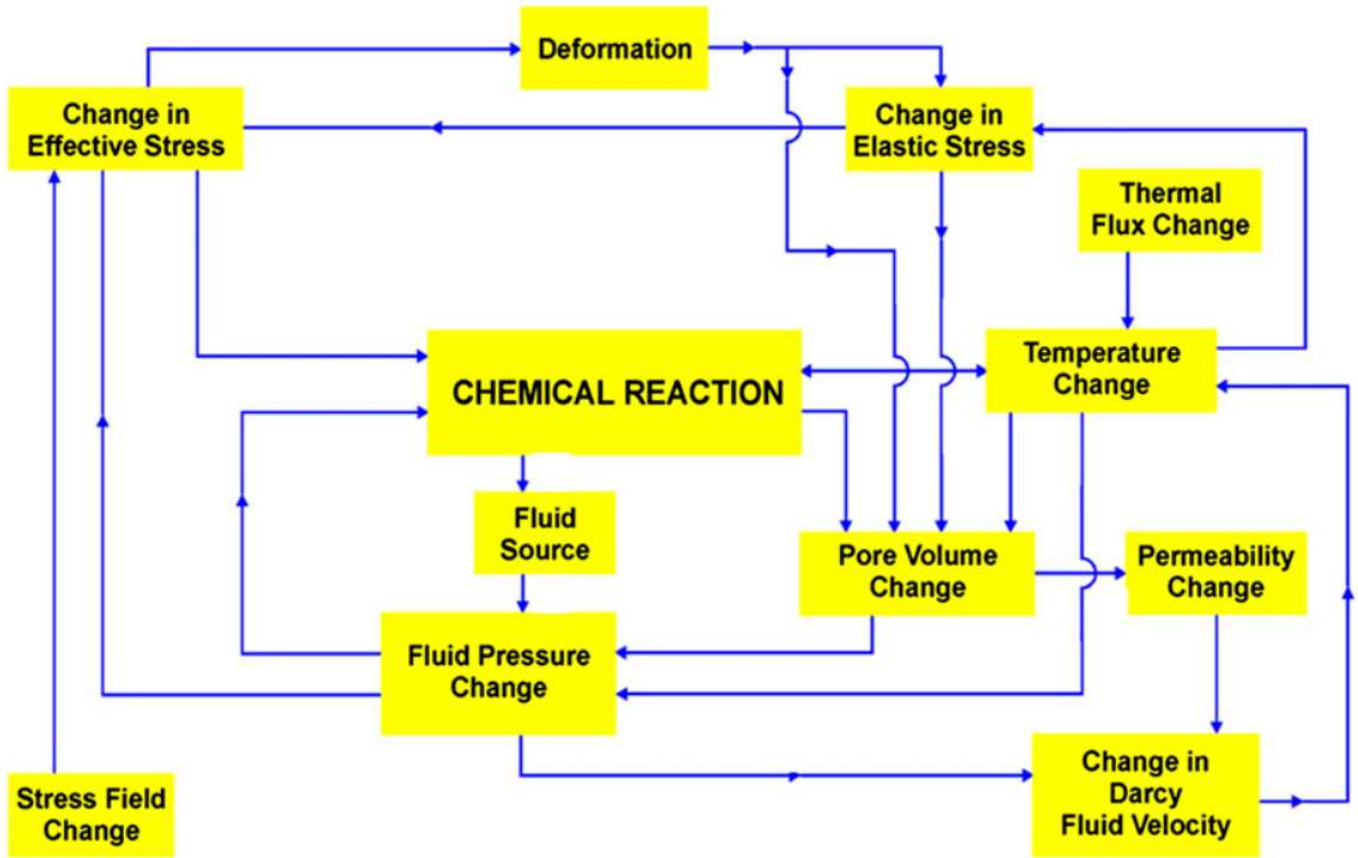


Figure 12

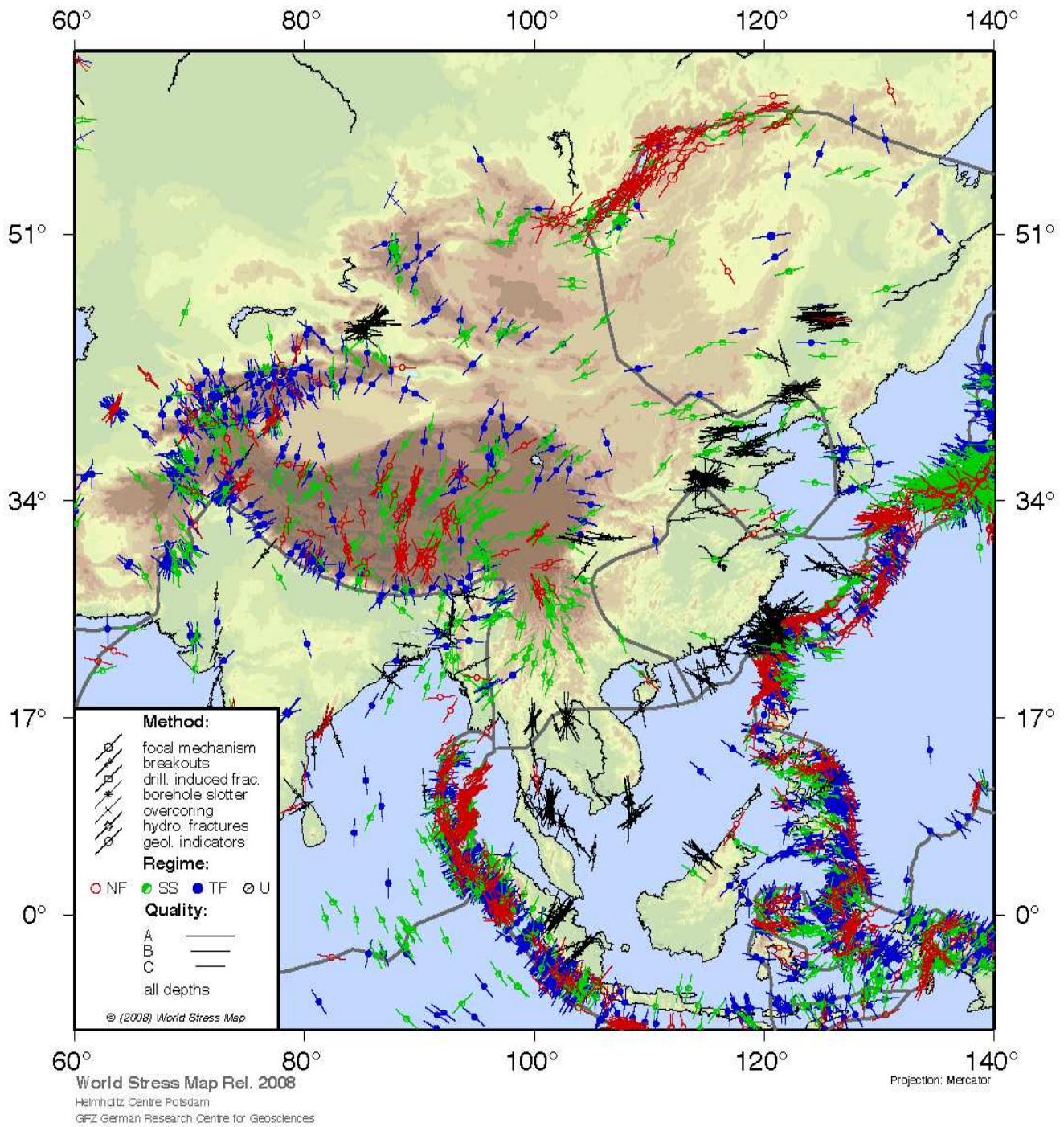


Figure 13

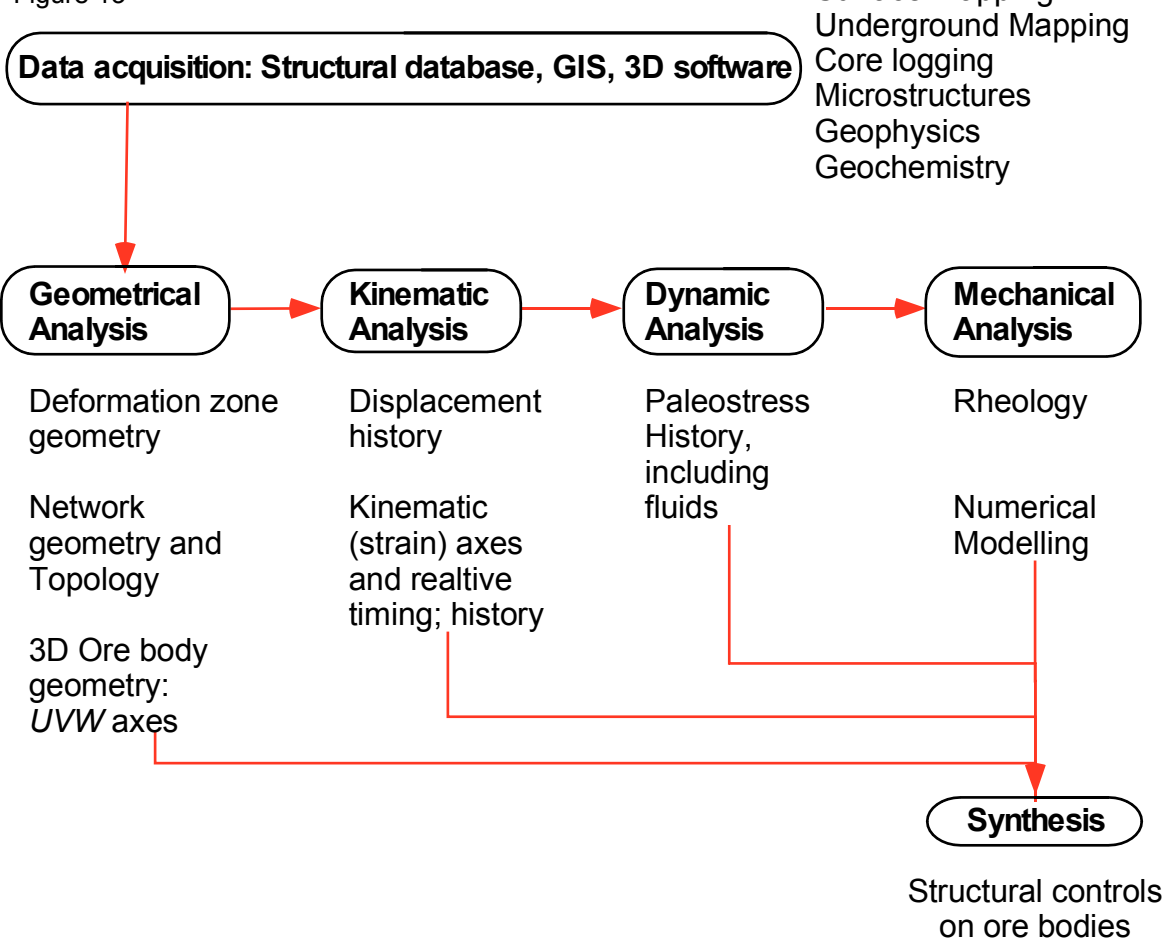




Table 1. Deformation and Intrusive events at Sunrise Dam Gold Mine, WA.

Event	Kinematics	Regime	$\sigma_1$	$\phi$
<b>Extension</b>	E-W extension			
<b>D6?</b>	Dextral conjugate faulting			
<b>D5</b>	Sinistral faulting	Strike-slip	SE	0.95
<b>D4b</b>	Dextral faulting (late stage) Reactivation and extension			
<b>D4a</b>	Dextral faulting (early stage)	Strike-slip	ENE	0.95
<b>Porphyry</b>	Dyke Intrusion $2674 \pm 3$ Ma			
<b>D3</b>	Thrusting and sinistral wrenching	Strike-slip	SE	0.5
<b>Porphyry</b>				
<b>D2</b>	Regional EW shortening			
<b>D1</b>	NW thrusting or extension			